100 μmol/L chloroquine (Sigma-Aldrich, St Louis, MO), 100 μmol/L RO-31-8220 (Calbiochem), 100 μmol/L staurosporine (Calbiochem), 1 μmol/L UO126 (Calbiochem), 30 mmol/L LiCl (Sigma-Aldrich), 30 mmol/L kenpaullone (Calbiochem), or 5 μmol/L BIO (Calbiochem).

For siRNA experiments, SW480 cells were transfected with 100 nmol/L siRNA oligonucleotide along with 1 μg of pCMV-Flag-WT-Hath1 for 12 hours, cultured for an additional 12 hours under the usual conditions, and then treated with MG132 or left untreated for 12 hours. A siRNA oligonucleotide specific for human GSK3β was obtained from Santa Cruz Biotechnology (Santa Cruz, CA), and a negative control (nonsense siRNA) oligonucleotide was synthesized as described elsewhere.[24] After transfection, cells were harvested, washed with phosphate-buffered saline (PBS) once, and incubated on ice for 15 minutes in 1% sodium dodecyl sulfate (SDS)-containing radioimmunoprecipitation assay (RIPA) buffer (10 mM Tris-HCl [pH 8.0], 1% Triton X-100, 1% SDS, 0.1% sodium deoxycholate, 1 mmol/L EDTA, 0.5 mmol/L ethylene glycol-bis(β-aminoethyl ether)-*N,N,N′,N′*-tetraacetic acid, and 140 mmol/L NaCl). After brief sonication of the lysates to shear genomic DNA, the samples were centrifuged for 20 minutes and the supernatant was used as whole cell extract. The protein concentration in each sample was determined by using protein assay reagent (Pierce, Rockford, IL). For immunoblotting, 50 μg or 100 μg of whole cell extract was separated in 12% SDS-polyacrylamide gels, transferred to polyvinylidene difluoride membranes, blocked, and probed according to standard procedures.[24] The following antibodies and dilutions were used: mouse anti-Flag M2 (Sigma Chemical Co, St Louis, MO), 1:5000; mouse anti-dephospho-β-catenin (Alexis, San Diego, CA), 1:500; mouse anti-GSK3 (Calbiochem), 1:1000; rabbit anti-USF2 (loading control for the amount of nuclear proteins; Santa Cruz Biotechnology), 1:1000; and mouse anti-β-actin (loading control for the whole cell extracts; Sigma Chemical Co), 1:5000. Horseradish peroxidase-conjugated secondary antibodies were used for mouse (Amersham Biosciences UK, Buckinghamshire, England) and rabbit immunoglobulin G (Cell Signaling Technology, Danvers, MA). Blots were visualized with the ECL Plus System (Amersham Biosciences UK) by using a Lumi-Imager F1 system (Roche Diagnostics, Rotkreutz, Switzerland). For immunoprecipitation assays, 300 μg of whole cell extract in 1% SDS-containing RIPA buffer was diluted with 9 vol of non-SDS-containing RIPA buffer to give an SDS concentration of 0.1%, and then the total volume was adjusted to 1 mL by adding an appropriate amount of 0.1% SDS-containing RIPA buffer. The lysates were precleared by incubation with 40 μL of protein G/Sepharose (50% slurry in 0.1% SDS-RIPA buffer) for 1 hour, and then the supernatants were incubated with 1 μg of anti-Flag M2 antibody (Sigma Chemical Co) overnight. A 40-μL aliquot of 50% protein G/Sepharose slurry was added to each sample and incubated for 2 hours at 4°C. Precipitates were washed 3 times in 0.1% SDS-containing RIPA buffer, resolved by SDS/polyacrylamide gel electrophoresis, and analyzed by immunoblotting using a mouse anti-myc antibody (Invitrogen, Carlsbad, CA) at 1:1000 dilution. Protein visualization was performed as described previously.

Semiquantitative Reverse-Transcription PCR and Northern Blotting

Total RNA was isolated by using TRIzol reagent (Invitrogen). Aliquots of 5 μg of total RNA were used for complementary DNA synthesis in 21 μL of reaction volume by using oligo dT primers. One microliter of complementary DNA was amplified with 0.25 U of LA Taq polymerase (Takara Bio, Otsu, Japan) in a 25-μL reaction. Sense and antisense primers and the cycle numbers for the amplification of each gene were as follows: sense Flag, 5′-CACCATGGATTACAAGGATGACGACGAT-3′ and antisense Hath1, 5′-TTGCCCGCGCCCCCTTCATAG-3′ for the fragment covering the region for Flag-Hath1 (20 cycles); sense Flag, 5′-CACCATGGATTACAAGGATGACGACGAT-3′ (common for the S primer for the Flag-Hath1 fragment) and antisense Flag-EGFP, 5′-AGGATGTTGCCGTCCTCC-3′ for Flag-EGFP (20 cycles); sense GSK3β, 5′-ATCTTAATCTGGTGCTGGACTATGT-3′ and antisense GSK3β, 5′-TTGAGTGGTGAAGTTGAAGAGTGCA-3′ for GSK3β (25 cycles); sense MUC2, 5′-CTGCACCAAGACCGTCCTCATG-3′ and antisense MUC2, 5′-GCAAGGACTGAACAAAGACTCAGAC-3′ for MUC2 (25 cycles); sense c-Myc, 5′-CTTCTGCTGGAGGCCACAGCAAACCTCCTC-3′ and antisense-c-Myc, 5′-CCAACTCCGGGATCTGGTCACGCAGGG -3′ for c-Myc (25 cycles); sense Hath1, 5′-AAGACGTTGCAGAAGAGACCCG-3′ and antisense Hath1, 5′- TTGCCCGCGCCCCCTTCATAG-3′ (common for the antisense primer for Flag-Hath1 fragment) for endogenous Hath1 (25 cycles); and sense glyceraldehyde-3-phosphate dehydrogenase (G3PDH), 5′-TGAAGGTCGGAGTCAACGGATTTGGT-3′ and antisense G3PDH, 5′-CATGTGGGCCATGAGGTCCACCAC-3′ for glyceraldehyde-3-phosphate dehydrogenase (17 cycles). The amplification for each gene was logarithmic under these conditions. PCR products were separated on 1.5% agarose gels, stained with ethidium bromide, and visualized with a Lumi-Imager F1 (Roche Diagnostics).

Expression levels of Hath1 mRNA in human tissues were analyzed by using 2 human multiple tissue blots (BioChain Institute, Hayward, CA). The complementary DNA probe corresponding to nucleotides +1/+749 for the *Hath1* gene was generated by reverse-transcription (RT)-PCR from an RNA sample obtained from human colonic tissues. The probe for G3PDH was also generated by RT-PCR. The probes were labeled with [α-32P]deoxycytidine triphosphate by random priming using RediPrime II (Amersham Biosciences UK) according to the

manufacturer's instructions. Hybridization was performed in Ultra Hyb solution (Ambion, Austin, TX) at 42°C overnight for Hath1 and at 55°C for 2 hours for β-actin. Visualization of the hybridized signals was conducted with the BAS-2000 image analyzing system (Fuji Film, Tokyo, Japan).

Reporter Assays

SW480 cells were transiently transfected with 10 ng of renilla luciferase reporter plasmid pRL-TK-Luc (Promega) along with 100 ng of either TOPflash, FOPflash, or an E-box-Luc reporter plasmid. One microgram of the expression plasmid pCMV-Flag-WT-Hath1 or its empty control, and the same amount of pCS2-APC2 or its empty control, were also cotransfected, keeping the total amount of plasmid per transfection constant. Transfections of 293T cells were performed identically, except for substituting the pCS2-APC2 with the pRL5-Wnt1 and the pCS2 vector with the pRL5 vector, respectively. After 12 hours of transfection, cells were cultured for 24 hours and lysed by 3 cycles of freezing and thawing. Firefly luciferase activity was normalized with renilla luciferase activity in each sample by using the Dual Luciferase Kit (Promega). The E-box-dependent luciferase activities were shown as arbitrary units normalized by renilla luciferase activity, and the β-catenin/TCF-dependent luciferase activities were shown as a ratio of TOPflash and FOPflash.

Immunocytochemistry

SW480 cells were cotransfected on a sterile glass coverslip with 1 μg of a bicistronic expression vector pMX-Flag-Hath1-IRES-GFP or its empty control together with 1 μg of a pCS2-APC2 or pCS2 vector as indicated. Twelve hours after transfection, cells were fixed with 4.0% paraformaldehyde, rinsed twice with PBS, and permeabilized with 0.2% Triton X-100 in PBS, followed by incubation for 1 hour in 3% bovine serum albumin-containing PBS to block nonspecific antibody binding. The samples were incubated for 3 hours at 37°C with either mouse anti-Flag antibody (1 μg/mL) or mouse anti-MUC2 antibody (1 μg/mL, Ccp58; Santa Cruz Biotechnology), washed twice with PBS, and then incubated for 1 hour at 37°C with Alexa 594-conjugated anti-mouse fluorescent secondary antibodies (Molecular Probes, Eugene, OR). The cells were also counterstained with 4′,6-diamidino-2-phenylindole (Vector Laboratories, Burlingame, CA) to visualize nuclei. The samples were washed 3 times with PBS and analyzed with an epifluorescence microscope (BX-50; Olympus, Tokyo, Japan) equipped with a PDMC device camera (Polaroid, Waltham, MA) for coexistence of the fluorescent signals of the secondary antibodies (Flag-Hath1 or MUC2 protein) and green fluorescent protein, the latter of which is translated from the IRES element fused downstream of the coding region for Flag-Hath1 protein. Images were processed in Adobe Photoshop software (Adobe Systems Inc, San Jose, CA).

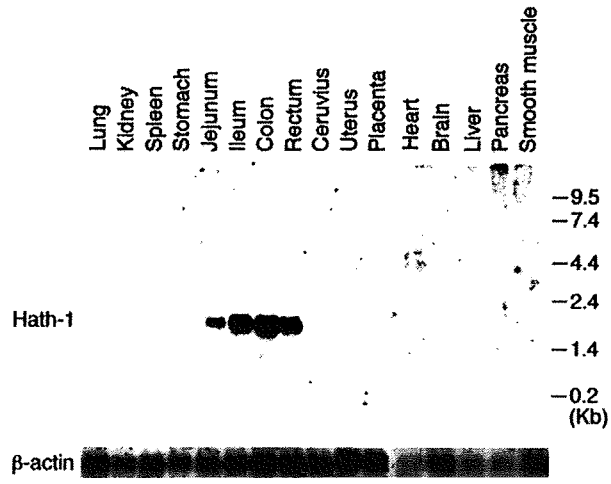

Figure 1. Expression of Hath1 mRNA is confined to the lower gastrointestinal tract. Hath1 mRNA expression in various adult human tissues was analyzed by Northern blotting by using a complementary DNA probe corresponding to nucleotides +1/+749 of the *Hath1* gene. Hybridization with a probe for β-actin is shown as a loading control. Hath1 mRNA is indeed exclusively expressed in the gastrointestinal tract of the human adult body. Moreover, the amount of Hath1 mRNA expression within the gastrointestinal tract increases as it reaches downward to the anal verge, where the population of secretory lineage epithelial cells is also increased.

Immunohistochemistry

Normal and cancerous colonic mucosae were obtained from 4 patients with colorectal cancer who underwent colectomy. Written informed consent was obtained from all patients, and these experiments were approved by the Tokyo Medical and Dental University Hospital Ethics Committee on Human Subjects. Immunohistochemistry for β-catenin was performed as described elsewhere,[25] using anti-β-catenin antibody (BD Transduction, San Diego, CA) and the standard ABC method (Vectastain; Vector Laboratories). Staining was developed by addition of diaminobenzidine (Vector Laboratories). Hath-1 antibody was generated by immunizing rabbits with Hath-1 peptide (247-265). Samples were fixed with 4% paraformaldehyde and subjected for staining using a TSA Signal Amplifying Kit (Molecular Probes) following the manufacturer's instructions. Staining was developed by addition of Alexa 488-conjugated tyramide. Sections were also counterstained with 4′,6-diamidino-2-phenylindole (Vector Laboratories) to visualize nuclei. Stained samples were analyzed with an epifluorescence microscope (BX-50; Olympus) equipped with a PDMC device camera (Polaroid).

Results

Expression of Hath1 mRNA Is Confined to the Lower Gastrointestinal Tract

The mRNA expression of Math1 and Hath1 is reported to be confined to the gastrointestinal tract in adult mice[26] and humans,[19] respectively. However, precise analysis of the expression of Hath1 mRNA within the gastrointestinal tract has never been reported. Thus, we compared mRNA expression of Hath1 in each section of the adult human gastrointestinal tract by Northern blotting. Results revealed that Hath1 mRNA is indeed exclusively expressed in the gastrointestinal tract, from the jejunum to the rectum (Figure 1). Moreover, the amount of Hath1 mRNA expression was significantly increased in the colon, compared with the jejunum or the ileum, where the population of secretory lineage epithelial cells is relatively increased. These results suggested that Hath1 expression is strictly regulated by mRNA expression, at least in the normal adult human body, and may have critical roles especially in the differentiation of colonocytes into secretory lineage cells.

Hath1 Undergoes Proteasome-Mediated Proteolysis in Human Colon Cancer–Derived Cells

To further analyze the functional role of Hath1 in colonocyte differentiation, we first asked whether an overexpression of Hath1 could change any phenotype of human colon-derived epithelial cells. Because the results of the former section suggested that expression of Hath1 mRNA may directly lead to Hath1 protein

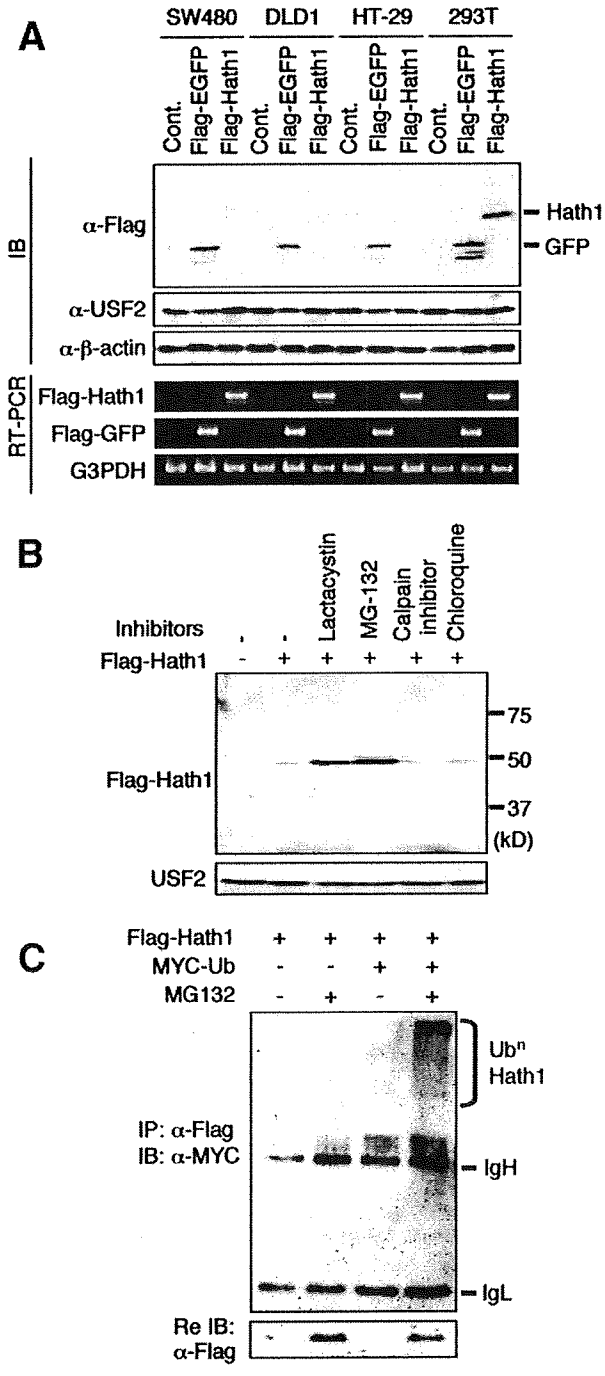

Figure 2. Hath1 undergoes proteasome-mediated proteolysis in human colon cancer–derived cells. (*A*) Hath1 protein expression cannot be detected after introduction of a gene encoding Hath1 in human colon cancer–derived cells. An expression plasmid encoding either Flag-tagged WT-Hath1 (Flag-Hath1), Flag-tagged EGFP (Flag-EGFP), or an empty control (Cont.) was transfected into human colon cancer–derived cell lines (SW480, DLD-1, and HT-29) or a noncolonic cell line (293T). Introduction of the genes was confirmed by semiquantitative RT-PCR, and the expression of the corresponding protein was examined by immunoblot (IB). While Flag-tagged EGFP shows stable expression of both mRNA and protein in every cell line, protein expression of Flag-Hath1 is detectable in 293T cells but not in colon cancer cell lines. Semiquantitative RT-PCR shows an equal amount of Flag-Hath1 mRNA expression in both 293T cells and colon cancer cell lines. (*B*) Hath1 protein is degradated by a proteasome-mediated mechanism in colon cancer cells. Flag-WT-Hath1 (Flag-Hath1) expression vector was transfected into SW480 cells and treated with various inhibitors of cellular proteolytic systems during protein expression. Expression of FLAG-Hath1 protein was examined by immunoblot using anti-Flag antibodies. Only the inhibitors of the proteasome pathway (lactacystin and MG132), but not any other inhibitor of the proteolytic pathway (calpain inhibitor and chloroquine), significantly increased protein expression of FLAG-Hath1. (*C*) Hath1 protein is polyubiquitinated in colon cancer cells. Expression vectors for Flag-Hath1 and Myc-tagged ubiquitin (Myc-Ub) were cotransfected into SW480 cells. Following transfection, cells were treated with or without MG132 during protein expression. The lysates were immunoprecipitated (IP) with anti-Flag antibodies and subjected to immunoblot (IB) using anti-Myc antibodies. Cotransfection of Flag-Hath1 and Myc-Ub, followed by inhibition of the proteasome pathway by MG132, allowed detection of the stabilized, polyubiquitinated FLAG-Hath1 protein by anti-myc antibody. Two bands labeled as IgH and IgL represent heavy chain and light chain of anti-Flag antibody used for immunoprecipitation, respectively. Reprobing the same membrane (Re IB) with anti-FLAG antibody shows efficient immunoprecipitation of FLAG-Hath1 protein only in MG132-treated conditions, because FLAG-Hath1 proteins are readily ubiquitinated and degradated in other conditions.

expression and function to regulate differentiation in colonocytes, we introduced an expression plasmid vector encoding Flag-tagged Hath1 (Flag-WT-Hath1) into various human colon cancer–derived epithelial cell lines. Surprisingly, significant expression of FLAG-Hath1 protein could not be observed in all 3 colon cancer cell lines examined, which were SW480, DLD1, and HT-29. This was not due to low efficiency of transfection or poor sensitivity of the immunoblot, because expression of Flag-EGFP protein could be easily detected by introducing the same amount of the expression plasmid having the same plasmid backbone (Figure 2*A*). Furthermore, semiquantitative RT-PCR showed an equal amount of Flag-Hath1 or Flag-EGFP mRNA expression in every colon cancer cell line, confirming the efficient transfection of the FLAG-Hath1 gene. However, Flag-Hath1 and Flag-EGFP showed equal expression of both mRNA and protein in 293T cells. These results suggested that there might be a posttranscriptional regulation of Hath1 expression involving protein degradation, specifically in colon cancer cells (Figure 2*A*). To confirm the involvement of proteolysis in the significantly decreased expression of Hath1 protein in colon cancer cell lines, we used various pharmacologic inhibitors of the cellular proteolytic system. When SW480 cells were treated with these inhibitors after transfection of Flag-Hath1 expression vectors, inhibitors such as calpain inhibitor or chloroquine had no effect on protein expression of Flag-Hath1 (Figure 2*B*). In sharp contrast, treatment with proteasome inhibitors such as MG132 or lactacystin significantly increased the protein expression of Flag-Hath1, suggesting that Hath1 protein is degradated by the proteasome-mediated proteolysis in colon cancer cells (Figure 2*B*). Because proteasome-mediated proteolysis often requires conjugation of ubiquitins to the target protein,[27,28] we next examined whether Hath1 proteins are ubiquitinated before degradation in

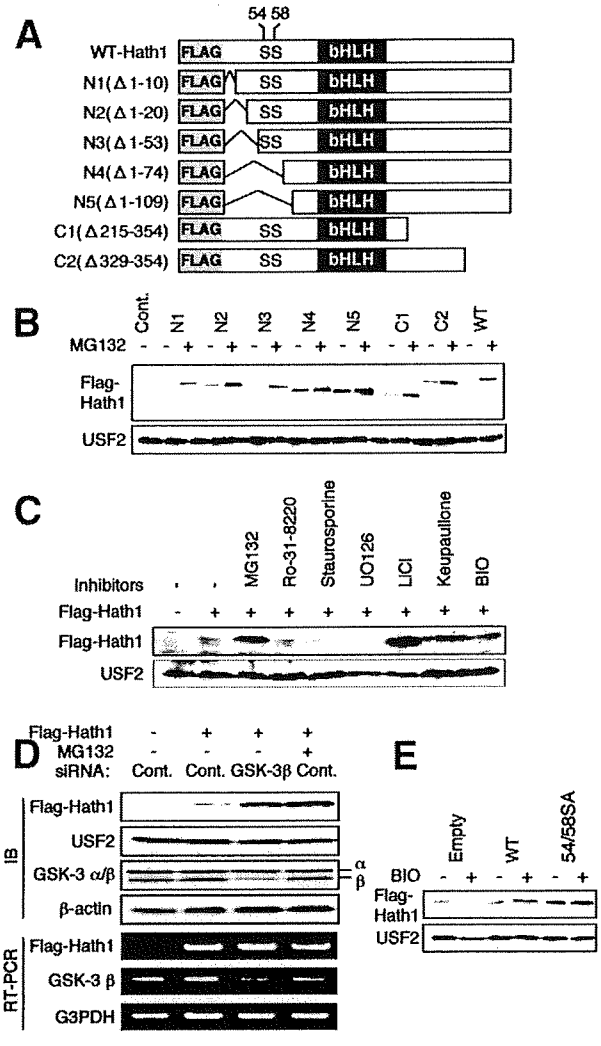

Figure 3. GSK3β-mediated Hath1 proteolysis in colon cancer cells critically requires S54 and S58 of Hath1 protein. (*A*) Schematic representation of various FLAG-tagged Hath1 mutants. Deletion mutants of the N-terminal or C-terminal part of the Hath1 protein are designated as N1–N4 or C1 and C2 mutants. The deleted region of each mutant is designated by amino acid numbers, that is, Δ1–10 designates deletion of amino acid 1–10 of Hath1 protein. The basic helix-loop-helix domain located in the central region as well as 2 serine (S) residues at positions 54 (S54) and 58 (S58) are shown. (*B*) The region consisting of amino acids 54–74 is required for active degradation of Hath1 protein. The wild-type and mutant Hath1 protein shown in *A* were expressed with or without MG132 treatment in SW480 cells. Protein expression was detected by immunoblot using anti-FLAG antibody. N4 and N5 mutant, but not any other wild-type or mutant Hath1 protein, showed no difference in the amount of protein expression between MG132-treated or untreated conditions. (*C*) Proteolysis of Hath1 is suppressed by specific inhibitors of GSK3β in colon cancer cells. Flag-WT-Hath1 was transfected into SW480 cells and treated with various protein kinase inhibitors. Protein expression was detected by immunoblot using anti-FLAG antibody. FLAG-Hath1 protein is stabilized by the proteasome inhibitor (MG132) and kinase inhibitors specific for GSK3β (LiCl, kenpaullone, BIO) but not by other kinase inhibitors (Ro-31-8220, staurosporine, UO126). (*D*) Gene silencing of GSK3β by siRNA increases Hath1 protein expression. An siRNA specific for GSK3β was cotransfected with Flag-WT-Hath1 into SW480 cells. Transfection of a nonsense siRNA served as a control (Cont.). Expression of FLAG-Hath1 and GSK3β was analyzed by semiquantitative RT-PCR and immunoblotting. Transfection of a GSK3β-specific siRNA significantly reduced both mRNA and protein expression of GSK3β. The specific knockdown of GSK3β increased protein expression of cotransfected FLAG-Hath1, which could also be induced up to a similar level by MG132 treatment. (*E*) S54 and S58 are the critical residues for GSK3β-mediated Hath1 proteolysis. An empty vector encoding no protein (*Empty*), or FLAG-tagged, wild-type (WT), or 54/58 SA mutant of Hath1 (54/58SA), in which both S54 and S58 of the Hath1 protein were substituted to alanines, was transfected into SW480 cells. The effect of treatment with a GSK3β-specific inhibitor (BIO) on the expression of each protein in SW480 cells was examined by immunoblot. 54/58 SA mutant of Hath1, but not the WT, showed stable protein expression without BIO treatment. A trace signal examined in the left end of the "Flag-Hath1" blot has been determined to be a nonspecific signal and does not represent expression of a Flag-tagged protein.

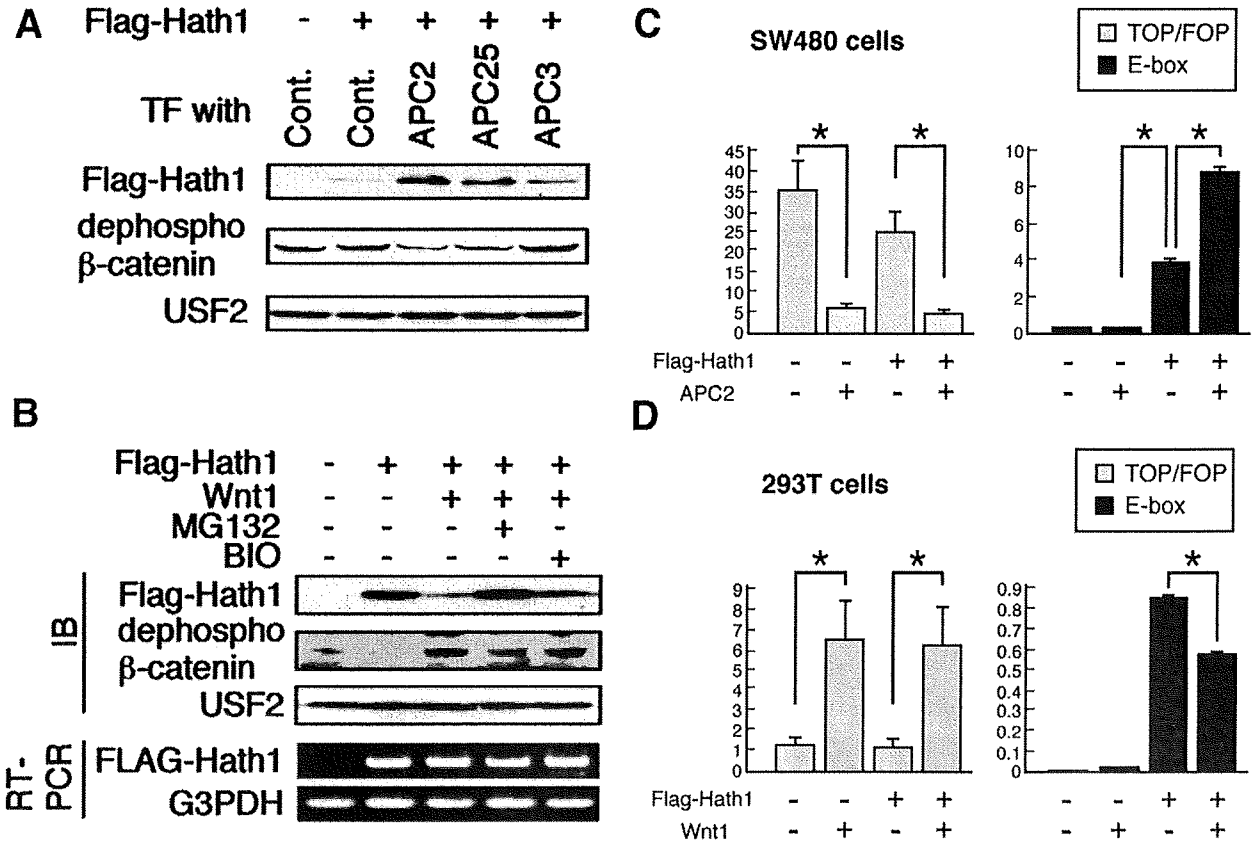

Figure 4. The canonical Wnt pathway reciprocally regulates Hath1 and β-catenin protein stability and downstream transcription activities via GSK3β. (*A*) Suppression of Wnt signaling in colon cancer cells increases expression of Hath1 protein. Flag-WT-Hath1 and APC mutants that are capable (APC2 and APC25) or incapable (APC3) of destabilizing β-catenin were cotransfected into SW480 cells. Cell lysates were subjected to immunoblotting for Flag-Hath1 (anti-Flag) or dephosphorylated β-catenin. Cotransfection of APC2 or APC25, but not of APC3, reduced the amount of dephosphorylated β-catenin protein and conversely increased the amount of Hath1 protein. (*B*) Activation of Wnt signaling induces degradation of Hath1 protein. Expression vectors for Flag-Hath1 and Wnt1 were cotransfected into 293T cells. Cells were cultured with or without MG132 or BIO, and protein expression of Hath1 and dephosphorylated β-catenin was analyzed by immunoblotting (IB). Equivalent transfection of Flag-Hath1 was confirmed by semiquantitative RT-PCR. Expression of Wnt1 in 293T cells induced dephosphorylation of β-catenin protein and also reduced expression of the cotransfected Flag-Hath1 protein (*lane 3*). This reduction of Flag-Hath1 protein is rescued by addition of a proteasome inhibitor (MG132) or a specific inhibitor of GSK3 (BIO). (*C*) Suppression of Wnt signaling in colon cancer cells up-regulates Hath1-mediated, E-box–dependent transcription and reciprocally down-regulates β-catenin/TCF–dependent transcription. Flag-WT-Hath, APC2, and designated reporter constructs were cotransfected into SW480 cells. E-box–dependent luciferase activities were shown as arbitrary units after normalization by renilla luciferase activity, and β-catenin/TCF–dependent luciferase activities are shown as a ratio of TOPflash and FOPflash. *$P < .005$. Transfection of APC2 significantly down-regulated β-catenin/TCF–dependent transcription but conversely up-regulated Hath1-mediated, E-box–dependent transcription in SW480 cells. (*D*) Activation of Wnt signaling in 293T cells down-regulates Hath1-mediated, E-box–dependent transcription and reciprocally up-regulates β-catenin/TCF–dependent transcription. Flag-WT-Hath, Wnt1, and designated reporter constructs were cotransfected into 293T cells. E-box– and β-catenin/TCF–dependent transcriptional activities were measured as described in the former section. *$P < .005$. Transfection of Wnt1 significantly up-regulated β-catenin/TCF–dependent transcription but conversely down-regulated Hath1-mediated, E-box–dependent transcription in 293T cells.

SW480 cells. For this purpose, Myc-tagged ubiquitin and Flag-Hath1 were coexpressed in SW480 cells and, subsequently, proteasome-mediated degradation was inhibited by MG132. When the cell lysates were immunoprecipitated by anti-Flag antibody, conjugation of Myc-tagged ubiquitin to Flag-Hath1 protein was detectable by immunoblot using anti-Myc antibody (Figure 2*C*). Ubiquitinated Hath1 protein appeared as a broad band on the membrane, suggesting that it is conjugated with random numbers of multiple ubiquitins (polyubiquitinated). Reprobing the same membrane (Re IB) with anti-FLAG antibody showed efficient immunoprecipitation of FLAG-Hath1 protein only in MG132-treated conditions, because FLAG-Hath1 proteins are readily ubiquitinated and degradated in other conditions (Figure 2*C*). These results collectively suggested that Hath1 proteins are polyubiquitinated before degradation by the proteasome-mediated proteolysis in colon cancer cells.

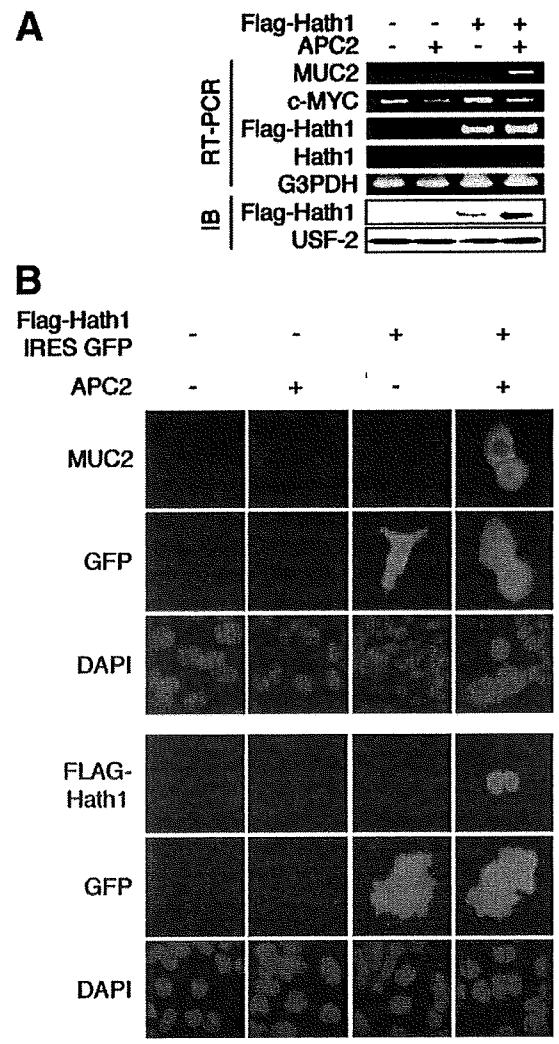

Figure 5. Inactivation of canonical Wnt signaling is required for Hath1-mediated colonocyte differentiation. (*A*) Suppression of canonical Wnt signaling in colon cancer cells is required for Hath1-mediated colonocyte differentiation. Expression plasmids for Flag-Hath1 and APC2 were cotransfected into SW480 cells. Expression of MUC2, C-MYC, Flag-Hath1, endogenous Hath1 (Hath1), and G3PDH mRNA was analyzed by RT-PCR. In the same experiment, protein expression of Flag-Hath1 and USF2 was examined by immunoblotting (IB). The expression of the goblet cell–specific gene *MUC2* was induced only when both FLAG-Hath1 and APC2 were expressed in SW480 cells. (*B*) MUC2 protein is expressed in cells that Hath1 protein stabilized by suppression of Wnt signaling. A bicistronic expression vector pMX-Flag-Hath1-IRES-GFP or its empty control was cotransfected with an expression vector for APC2 into SW480 cells. Cells were stained by fluorescent immunocytochemistry for MUC2 (*upper half, red*) or Flag-Hath1 (*lower half, red*). The green signal of green fluorescent protein (GFP) represents transcription of Flag-Hath1, encoded upstream of GFP and the IRES element. Expression of MUC2 protein is induced only when FLAG-Hath1 protein is stabilized by cotransfecting FLAG-Hath1 and APC2 into SW480 cells. DAPI, 4′,6-diamidino-2-phenylindole.

GSK3β-Mediated Hath1 Proteolysis in Colon Cancer Cells Critically Requires S54 and S58 of Hath1 Protein

Former results confirmed that Hath1 protein is constitutively degradated by proteasome-mediated proteolysis in colon cancer cells. This raised the question whether there is a specific region within the Hath1 protein that is critically required for the present proteolysis system. Although it is well known that Hath1 protein contains a basic helix-loop-helix domain that is critically required for binding to the target sequence of DNA,[26,29] other regions of the protein have not been functionally characterized. To determine the region that may be critically required for the degradation of Hath1 protein, various mutants of Flag-tagged Hath1 protein (Figure 3*A*) were expressed in SW480 cells (Figure 3*B*). Immunoblot using anti-Flag antibody revealed that, although a trace amount of Flag-tagged protein was detected without MG132 treatment by increasing the amount of loaded lysates, deleting up to 53 amino acids of the N-terminal end (N1 to N3), or 140 amino acids of the C-terminal end (C1 and C2), appeared to have no effect on protein stability of the Hath1 protein. However, deletions up to 74 or 109 amino acids of the N-terminal end (N4 and N5) showed markedly stable expression of Hath1 protein without MG132 treatment. These results indicated that the region between amino acids 54 and 74 is critically required for proteasome-mediated Hath1 proteolysis.

The region between amino acids 54 and 74 of the Hath1 protein included 2 serine and 3 threonine residues. It is well known that one of the important mechanisms required for proteasome-dependent degradation is the phosphorylation of specific amino acid residues.[30,31] Based on these data, we searched, using Scansite software (Scansite, Boston, MA), for whether a putative phosphorylation site may exist within the region between amino acids 54 and 74 of the Hath1 protein. Surprisingly, a distinct site extending from serine residue at position 54 (S54) to position 58 (S58) matched the consensus substrate sequence (S/T-X-X-X-S/T) for GSK3β (Figure 3*A*). These results raised a possibility that Hath1 protein is a substrate of GSK3β, and therefore Hath1 protein degradation is regulated by the phosphorylation of specific serine residues by GSK3β. To determine whether kinase activity of GSK3β is required for Hath1 protein degradation, SW480 cells were treated with inhibitors of various protein kinases and examined for FLAG-Hath1 protein expression by immunoblot (Figure 3*C*). Confirming the in silico search for putative phosphorylation sites, FLAG-Hath1 protein was stabilized by the proteasome inhibitor, MG132, and kinase inhibitors specific for GSK3β such as LiCl, kenpaullone, and BIO, but not by other kinase inhibitors such as Ro-31-8220, staurosporine, or UO126, which does not inhibit GSK3β.

To further confirm the involvement of GSK3β in Hath1 proteolysis, we used an siRNA-mediated gene knockdown system to specifically knock down GSK3β gene expression in colon cancer cells. Transfection of GSK3β-specific siRNA into SW480 cells successfully decreased both mRNA and protein expression of GSK3β in SW480 cells (Figure 3*D*). Under this condition, expression of the cotransfected Flag-Hath1 protein was significantly increased up to a comparable level with MG132 treatment. No change was observed in the quantity of Flag-Hath1 mRNA, suggesting that the increase of Flag-Hath1 protein is due to increased protein stability. These results further confirmed that kinase activity of GSK3β is critically required for Hath1 protein degradation in colon cancer cells.

We next examined whether the 2 serine residues found in the putative GSK3β target region (S54 and S58) are critically required for GSK3β-mediated Hath1 proteolysis. For this purpose, a mutant Flag-Hath1 in which 2 serine residues (S54 and S58) were replaced into 2 alanines (54/58SA) was expressed in SW480 cells. Consistently, examination of protein expression by immunoblot revealed that the 54/58 SA mutant of Hath1 (54/58SA), but not the wild type, showed stable protein expression without inhibition of GSK3β by BIO treatment.

These data collectively indicated that the kinase activity of GSK3β is critically required for the degradation of Hath1 in colon cancer cells and also that the 54th and 58th serine residues of the Hath1 protein are critically required for GSK3β-mediated Hath1 proteolysis.

The Canonical Wnt Pathway Reciprocally Regulates Hath1 and β-catenin Protein Stability and Downstream Transcription Activities via GSK3β

Former findings raised an important question as to how the kinase function of GSK3β for Hath1 proteolysis is regulated by the upstream signaling events in colon cancer cells. GSK3β is known to participate not only in the canonical Wnt pathway but also in other pathways such as insulin signaling.[32] However, it is also known that the kinase activity of GSK3β is regulated by a single signaling pathway within a single cell and is usually not modified or affected by multiple pathways.[33] In most human colorectal cancer cells, Wnt signal is aberrantly activated by various gene mutations. Indeed, all the colon cancer cell lines used in this study harbor mutations in the *APC* gene, which suppress the kinase activity of GSK3β on β-catenin phosphorylation and consequently stabilize β-catenin protein.[18] Moreover, a recent study showed that the Wnt signal activates GSK3 to phosphorylate LRP6 in opposite relationship to β-catenin.[34] Therefore, we hypothesized that GSK3β kinase activity is dominantly regulated by Wnt signaling in colon cancer cells, and the aberrant activation of this signal may be involved in Hath1 protein degradation via GSK3β. To confirm the hypothesis, we first examined whether Hath1 protein may be stabilized by the inactivation of the aberrant Wnt signaling in colon cancer cells. For this purpose, we used SW480 cells, in which aberrant Wnt signaling is caused by truncated mutation of *APC*. When the aberrant Wnt signaling of SW480 cells was

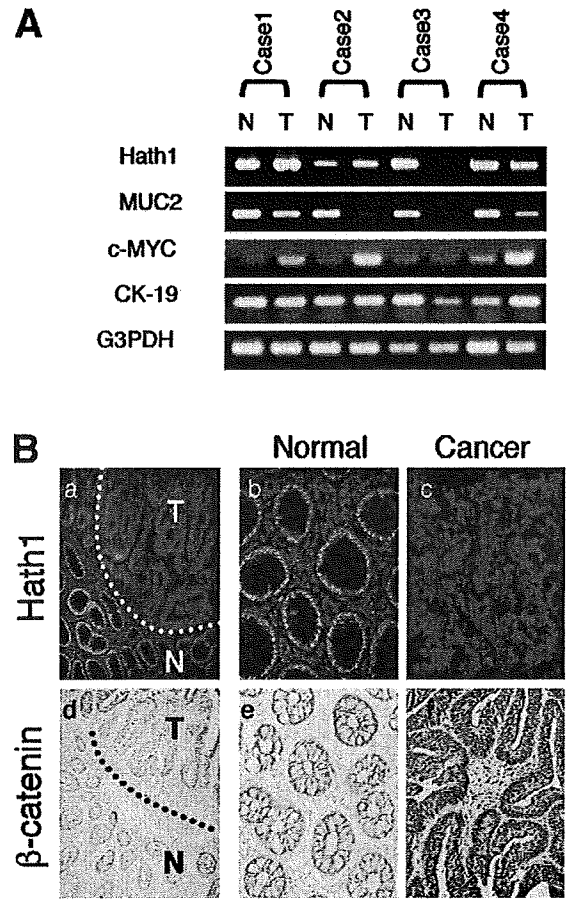

Figure 6. Hath1 protein expression is decreased in human colon cancer tissues expressing Hath1 mRNA and nuclear-located β-catenin protein. (*A*) Hath1 mRNA is expressed in both normal and cancer tissues of human colon. Four cases of colorectal cancer were examined (cases 1–4). N, normal colon mucosa; T, colon cancer tissue of each patient. Semiquantitative analysis of Hath1, C-MYC, MUC2, CK-19, and G3PDH mRNA expression was performed by RT-PCR. CK-19 served as a control for epithelial cell population, whereas G3PDH served as a loading control. In cases 1, 2, and 4, Hath1 mRNA is expressed in both normal and cancer tissue. (*B*) Hath1 protein expression is decreased in colon cancer tissue. The border lesion of the tumor in case 2 was subjected to immunohistochemical analysis. A lower magnification of the border lesion of the tumor (*a* and *d*) and also the magnified view of the cancer tissue (*c* and *f*) and the adjacent normal mucosa (*b* and *e*) are presented. Tissue sections were stained with either anti-Hath1 (Alexa 488, green signal, *a–c*) or anti–β-catenin (diaminobenzidine, brown signal, *d–f*). The figures show a significant decrease of Hath1 staining in cancer tissues compared with normal colonic mucosa, whereas nuclear located β-catenin is significantly increased in cancer tissues (original magnification: *a* and *d*, 100×; *b*, *c*, *e*, and *f*, 400×).

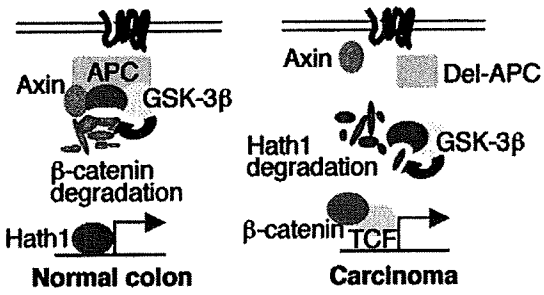

Figure 7. Schematic representation of Wnt-GSK3β–mediated regulation of colonocyte differentiation and proliferation. In normal colonocytes, differentiation is accelerated by turning off the Wnt signaling, which leads to GSK3β-mediated degradation of β-catenin protein and up-regulation of Hath1-mediated transcription of yet-unknown target genes. Conversely, during transformation of colonocytes into carcinoma cells, proliferation is accelerated by constitutive activation of Wnt signaling, which leads to GSK3β-mediated degradation of Hath1 protein and up-regulation of β-catenin/TCF–mediated transcription.

inactivated by transfecting APC mutants (APC2 and APC25) that are capable of forming complexes with β-catenin, Axin, and GSK3β,[22] the amount of endogenous dephosphorylated β-catenin as a stabilized form of β-catenin was significantly decreased but, surprisingly, the expression of cotransfected Flag-WT-Hath1 protein was significantly increased (Figure 4*A*). Transfection of the C-terminal fragment of human APC (APC3; amino acids 2130–2843) that is incapable of forming complexes with β-catenin, Axin, and GSK3β[22] into SW480 cells had no effect on both β-catenin phosphorylation and Flag-Hath1 protein stability (Figure 4*A*). This reciprocal regulation of Hath1 and β-catenin protein stability by Wnt signaling was also observed in 293T cells, in which Wnt signaling is usually inactivated. Activation of Wnt signaling in 293T cells by overexpression of the *Wnt1* gene resulted in a significant increase of the endogenous dephosphorylated, stabilized form of β-catenin protein and also a significant decrease in Flag-Hath1 protein expression. Treatment with MG132 or BIO completely restored the reduction of Flag-Hath1 protein expression induced by activation of Wnt signaling in 293T cells, suggesting that proteasome-mediated Hath1 proteolysis is regulated by the kinase activity of GSK-3β downstream of the canonical Wnt pathway (Figure 4*B*).

We further examined whether Wnt-GSK3β–mediated reciprocal regulation of Hath1 and β-catenin protein stability may also change the transcriptional activity of the corresponding downstream target genes of each protein. Consistent with previous reports,[22] expression of APC2 in SW480 cells decreased the ratio of TOPflash and FOPflash reporter activity by 0.14-fold, regardless of Flag-Hath1 cotransfection (Figure 4*C*). In sharp contrast, E-box–dependent reporter activity was increased by 2.3-fold by cotransfection of APC2 with Flag-Hath1 compared with single transfection of Flag-Hath1 into SW480 cells (Figure 4*C*). Thus, expression of APC2 in SW480 cells significantly down-regulated β-catenin/TCF–dependent transcription but conversely up-regulated Hath1-mediated, E-box–dependent transcription. In contrast, forced expression of *Wnt1* gene in 293T cells up-regulated the ratio of TOPflash and FOPflash reporter activity by 6-fold and, conversely, when Wnt1 was coexpressed with Flag-Hath1 in 293T cells, E-box–dependent reporter activity was down-regulated by 0.6-fold (Figure 4*D*). Thus, expression of Wnt1 in 293T cells significantly up-regulated β-catenin/TCF–dependent transcription but conversely down-regulated Hath1-mediated, E-box–dependent transcription. Single transfection of APC2 or Wnt1 does not change E-box–dependent transcription activity in both SW480 and 293T cells, suggesting that the observed E-box–dependent transcriptional activity represents Hath1-mediated transcription.

These data collectively indicated that GSK3β–mediated proteolysis of Hath1 protein observed in colon cancer cells is dependent on the aberrant activation of the canonical Wnt pathway and that GSK3β reciprocally regulates Hath1 and β-catenin protein stability in a Wnt-dependent manner, directly leading to significant changes in transcriptional activity of the downstream target genes.

Inactivation of Canonical Wnt Signaling Is Required for Hath1-Mediated Colonocyte Differentiation

It is well known that β-catenin/TCF–dependent transcription often promotes cell proliferation, whereas Hath1-dependent transcription promotes cell differentiation. Therefore, we next examined whether the Wnt-GSK3–mediated, reciprocal regulation of β-catenin and Hath1 protein stability and function may regulate the differentiation of colonocytes. For this purpose, we examined whether stabilization of Hath1 protein induced by inactivation of Wnt signaling may lead to spontaneous differentiation of poorly differentiated colon cancer cells. Consistent with former results, single transfection of APC2 into SW480 cells down-regulated mRNA expression of c-Myc but had no effect on colonocyte differentiation (Figure 5*A*). However, when Flag-Hath1 was cotransfected with APC2 in SW480 cells, Hath1 protein was stably expressed and subsequently induced expression of MUC2 mRNA, a specific marker for goblet cell differentiation.[35,36] Immunocytochemical analysis of Hath1 and MUC2 protein expression in SW480 cells showed that both stabilization of Flag-Hath1 protein and up-regulation of MUC2 protein expression were induced under the same condition (Figure 5*B*). Moreover, MUC2 protein was detected exclusively in green fluorescent protein–positive cells that were the bicistronic expression of *Flag-Hath1* gene, indicating that Hath1 protein caused the increase of MUC2 protein (Figure 5*B*).

Collectively, these results suggested that both inactivation of Wnt signaling and stable expression of Hath1

protein are required for colonocyte differentiation toward goblet cells.

A previous report showed that merely inactivating the aberrant Wnt signaling in HT-29 cells induced significant up-regulation of the *MUC2* gene.[19] In our experience, HT-29 cells are different from SW480 cells, because they readily express a small amount of Hath1 and MUC2 mRNA (data not shown). Thus, we speculate that inactivation of aberrant Wnt signaling in HT-29 cells may have up-regulated both mRNA expression and protein stability of the endogenous *Hath1* gene, leading to the significant up-regulation of MUC2 expression.

Hath1 Protein Expression Is Decreased in Human Colon Cancer Tissues Expressing Hath1 mRNA and Nuclear-Located β-catenin Protein

To reveal the role of Wnt-GSK3–mediated reciprocal proteolytic regulation of β-catenin and Hath1 in vivo, we analyzed the correlation between Hath1 mRNA, Hath1 protein, and nuclear localized β-catenin protein expression in human colon cancer tissues. In 3 of 4 cases, we found that tumor tissues expressed Hath1 mRNA at an amount comparable to the adjacent normal mucosa, as judged by RT-PCR (Figure 6*A*). Constitutive activation of Wnt signaling in cancer tissue of these cases was confirmed by the significant expression of *c-MYC*, one of the well-known target genes by β-catenin/TCF. Strikingly, in these cases, immunohistochemical analysis revealed that Hath1 protein is expressed in the normal mucosa but not in the tumor lesion (Figure 6*B*). In contrast, nuclear localized β-catenin protein was easily observed in the tumor lesion but was hardly found in the normal mucosa (Figure 6*B*). These data indicated that at least in some populations of colon cancers, Hath1 expression might be strictly suppressed by Wnt-mediated protein degradation, rather than the suppression of mRNA expression, thereby contributing to maintenance of the undifferentiated state of the tumor tissue.

Discussion

The present study describes a novel function of the canonical Wnt signaling, reciprocally regulating Hath1 and β-catenin protein stability via GSK3β (Figure 7). The "on" and "off" status of the Wnt signal directly converted the target of GSK3β between Hath1 and β-catenin protein, leading to subsequent protein degradation. Our results suggest that this mechanism not only regulates the amount of Hath1 and β-catenin protein expression but also contributes to the significant change in the expression of the downstream target genes and to the cell fate decision between cell differentiation and proliferation. Furthermore, our observations that the dysregulation of the Wnt pathway by components upstream of GSK3β, such as APC, not only contribute to the activation of β-catenin/TCF transcription but also induce concomitant destruction of the gut-specific transcription factor Hath1, provides new insights into the tissue-specific processes of colon cancer development.

It is known that the ubiquitin-proteasome pathway plays crucial roles in the carcinogenesis of some tissues by regulating the protein expression of transcriptional factors such as nuclear factor κB[37] and hypoxia-inducible factor 1.[38] However, our findings suggest that proteolytic regulation of Hath1 protein expression by the ubiquitin-proteasome pathway is a tissue-specific event observed exclusively in colon cancer cells. Moreover, the present system has an outstanding advantage for colon cancer carcinogenesis, in that a single mutation of an upstream gene in Wnt signaling could accelerate cell proliferation by β-catenin/TCF–dependent transcription and immediately shut down cell differentiation at the same time by rapid degradation of Hath1 protein, regardless of Hath1 mRNA expression. Therefore, the present function of the Wnt-GSK pathway further emphasizes the importance of aberrant Wnt signaling in colonocyte transformation.

This study also provides a new insight into the canonical Wnt pathway, because it indicates that GSK3β functions continuously, even when the upstream signal is inactivated, by changing its substrate specificity according to the upstream signal status. It is known that GSK3β changes target amino acid residue within a single substrate protein such as Map1b[39] and Snail,[40] depending on its upstream signals. Our study suggests for the first time that GSK3β could even change the substrate protein itself due to upstream Wnt signaling, leading to immediate degradation of the substrate protein by the ubiquitin-proteasome system. However, the present study could not provide precise evidence to understand whether Hath1 is directly phosphorylated by GSK3β or how changes of GSK3β target are sequentially regulated between Hath1 and β-catenin. In our recent study, in vitro kinase assay using recombinant Hath1 protein and activated GSK3β did not show any phosphorylation of Hath1 protein (data not shown). This result indicated that the phosphorylation of Hath1 might require specific adapter proteins such as Axin and APC to form a complex with GSK3β, as is the case with phosphorylation of β-catenin. However, so far we cannot completely exclude that the effect of GSK3β activity on Hath1 protein stability is possibly indirect. Overexpression of GSK3β had no effect on Hath1 and β-catenin protein stability, suggesting that the total amount of GSK3β protein is abundant enough and does not contribute to limit the substrate protein (data not shown). Thus, it is more likely that Wnt signal controls target specificity of the GSK3β by regulating the complex formation of the substrate with GSK3β and a yet-unknown adapter protein.

In summary, we showed for the first time a novel function of the Wnt-GSK3 signaling pathway, working as a molecular switch changing the cell fate between differentiation and proliferation by proteolytic, reciprocal reg-

ulation of Hath1 and β-catenin in colonocytes. Moreover, the aberrant Wnt signaling contributes to the carcinogenesis of colon cancers not only by the stabilization of β-catenin protein but also by the degradation of Hath1 protein in an intestine-specific manner. These findings provide better understanding of the molecular mechanism regulating Wnt-mediated carcinogenesis in colorectal cancers and further emphasize the importance of aberrant Wnt signaling in colonocyte transformation.

References

1. Booth C, Brady G, Potten CS. Crowd control in the crypt. Nat Med 2002;8:1360–1361.
2. El-Assal ON, Besner GE. HB-EGF enhances restitution after intestinal ischemia/reperfusion via PI3K/Akt and MEK/ERK1/2 activation. Gastroenterology 2005;129:609–625.
3. Haramis AP, Begthel H, van den Born M, van Es J, Jonkheer S, Offerhaus GJ, Clevers H. De novo crypt formation and juvenile polyposis on BMP inhibition in mouse intestine. Science 2004; 303:1684–1686.
4. Cheng H, Leblond CP. Origin, differentiation and renewal of the four main epithelial cell types in the mouse small intestine. V. Unitarian theory of the origin of the four epithelial cell types. Am J Anat 1974;141:537–561.
5. Gowan K, Helms AW, Hunsaker TL, Collisson T, Ebert PJ, Odom R, Johnson JE. Crossinhibitory activities of Ngn1 and Math1 allow specification of distinct dorsal interneurons. Neuron 2001;31: 219–232.
6. Ben-Arie N, Bellen HJ, Armstrong DL, McCall AE, Gordadze PR, Guo Q, Matzuk MM, Zoghbi HY. Math1 is essential for genesis of cerebellar granule neurons. Nature 1997;390:169–172.
7. Leonard JH, Cook AL, Van Gele M, Boyle GM, Inglis KJ, Speleman F, Sturm RA. Proneural and proneuroendocrine transcription factor expression in cutaneous mechanoreceptor (Merkel) cells and Merkel cell carcinoma. Int J Cancer 2002;101:103–110.
8. Bermingham NA, Hassan BA, Price SD, Vollrath MA, Ben-Arie N, Eatock RA, Bellen HJ, Lysakowski A, Zoghbi HY. Math1: an essential gene for the generation of inner ear hair cells. Science 1999;284:1837–1841.
9. Yang Q, Bermingham NA, Finegold MJ, Zoghbi HY. Requirement of Math1 for secretory cell lineage commitment in the mouse intestine. Science 2001;294:2155–2158.
10. Fre S, Huyghe M, Mourikis P, Robine S, Louvard D, Artavanis-Tsakonas S. Notch signals control the fate of immature progenitor cells in the intestine. Nature 2005;435:964–968.
11. Jensen J, Pedersen EE, Galante P, Hald J, Heller RS, Ishibashi M, Kageyama R, Guillemot F, Serup P, Madsen OD. Control of endodermal endocrine development by Hes-1. Nat Genet 2000; 24:36–44.
12. Sekine A, Akiyama Y, Yanagihara K, Yuasa Y. Hath1 up-regulates gastric mucin gene expression in gastric cells. Biochem Biophys Res Commun 2006;344:1166–1171.
13. Batlle E, Henderson JT, Beghtel H, van den Born MM, Sancho E, Huls G, Meeldijk J, Robertson J, van de Wetering M, Pawson T, Clevers H. Beta-catenin and TCF mediate cell positioning in the intestinal epithelium by controlling the expression of EphB/ephrinB. Cell 2002;111:251–263.
14. Huelsken J, Behrens J. The Wnt signalling pathway. J Cell Sci 2002;115:3977–3978.
15. Polakis P. Wnt signaling and cancer. Genes Dev 2000;14:1837–1851.
16. Marshman E, Booth C, Potten CS. The intestinal epithelial stem cell. Bioessays 2002;24:91–98.
17. Pinto D, Gregorieff A, Begthel H, Clevers H. Canonical Wnt signals are essential for homeostasis of the intestinal epithelium. Genes Dev 2003;17:1709–1713.
18. Polakis P. The oncogenic activation of beta-catenin. Curr Opin Genet Dev 1999;9:15–21.
19. Leow CC, Romero MS, Ross S, Polakis P, Gao WQ. Hath1, down-regulated in colon adenocarcinomas, inhibits proliferation and tumorigenesis of colon cancer cells. Cancer Res 2004;64: 6050–6057.
20. Shimura H, Hattori N, Kubo S, Mizuno Y, Asakawa S, Minoshima S, Shimizu N, Iwai K, Chiba T, Tanaka K, Suzuki T. Familial Parkinson disease gene product, parkin, is a ubiquitin-protein ligase. Nat Genet 2000;25:302–305.
21. Onishi M, Kinoshita S, Morikawa Y, Shibuya A, Phillips J, Lanier LL, Gorman DM, Nolan GP, Miyajima A, Kitamura T. Applications of retrovirus-mediated expression cloning. Exp Hematol 1996; 24:324–329.
22. Munemitsu S, Albert I, Souza B, Rubinfeld B, Polakis P. Regulation of intracellular beta-catenin levels by the adenomatous polyposis coli (APC) tumor-suppressor protein. Proc Natl Acad Sci U S A 1995;92:3046–3050.
23. Nishita M, Hashimoto MK, Ogata S, Laurent MN, Ueno N, Shibuya H, Cho KW. Interaction between Wnt and TGF-beta signalling pathways during formation of Spemann's organizer. Nature 2000;403:781–785.
24. Oshima S, Nakamura T, Namiki S, Okada E, Tsuchiya K, Okamoto R, Yamazaki M, Yokota T, Aida M, Yamaguchi Y, Kanai T, Handa H, Watanabe M. Interferon regulatory factor 1 (IRF-1) and IRF-2 distinctively up-regulate gene expression and production of interleukin-7 in human intestinal epithelial cells. Mol Cell Biol 2004; 24:6298–6310.
25. Matsumoto T, Okamoto R, Yajima T, Mori T, Okamoto S, Ikeda Y, Mukai M, Yamazaki M, Oshima S, Tsuchiya K, Nakamura T, Kanai T, Okano H, Inazawa J, Hibi T, Watanabe M. Increase of bone marrow-derived secretory lineage epithelial cells during regeneration in the human intestine. Gastroenterology 2005;128:1851–1867.
26. Akazawa C, Ishibashi M, Shimizu C, Nakanishi S, Kageyama R. A mammalian helix-loop-helix factor structurally related to the product of Drosophila proneural gene atonal is a positive transcriptional regulator expressed in the developing nervous system. J Biol Chem 1995;270:8730–8738.
27. Ciechanover A. The ubiquitin-proteasome proteolytic pathway. Cell 1994;79:13–21.
28. Hochstrasser M. Ubiquitin-dependent protein degradation. Annu Rev Genet 1996;30:405–439.
29. Massari ME, Murre C. Helix-loop-helix proteins: regulators of transcription in eucaryotic organisms. Mol Cell Biol 2000;20: 429–440.
30. Roos-Mattjus P, Sistonen L. The ubiquitin-proteasome pathway. Ann Med 2004;36:285–295.
31. Weissman AM. Themes and variations on ubiquitylation. Nat Rev Mol Cell Biol 2001;2:169–178.
32. Cross DA, Alessi DR, Cohen P, Andjelkovich M, Hemmings BA. Inhibition of glycogen synthase kinase-3 by insulin mediated by protein kinase B. Nature 1995;378:785–789.
33. Doble BW, Woodgett JR. GSK-3: tricks of the trade for a multitasking kinase. J Cell Sci 2003;116:1175–1186.
34. Zeng X, Tamai K, Doble B, Li S, Huang H, Habas R, Okamura H, Woodgett J, He X. A dual-kinase mechanism for Wnt co-receptor phosphorylation and activation. Nature 2005;438:873–877.
35. Chang SK, Dohrman AF, Basbaum CB, Ho SB, Tsuda T, Toribara NW, Gum JR, Kim YS. Localization of mucin (MUC2 and MUC3) messenger RNA and peptide expression in human normal intestine and colon cancer. Gastroenterology 1994;107:28–36.
36. Katz JP, Perreault N, Goldstein BG, Lee CS, Labosky PA, Yang VW, Kaestner KH. The zinc-finger transcription factor Klf4 is

required for terminal differentiation of goblet cells in the colon. Development 2002;129:2619–2628.
37. Greten FR, Eckmann L, Greten TF, Park JM, Li ZW, Egan LJ, Kagnoff MF, Karin M. IKK beta links inflammation and tumorigenesis in a mouse model of colitis-associated cancer. Cell 2004; 118:285–296.
38. Koshiji M, Kageyama Y, Pete EA, Horikawa I, Barrett JC, Huang LE. HIF-1 alpha induces cell cycle arrest by functionally counteracting Myc. EMBO J 2004;23:1949–1956.
39. Trivedi N, Marsh P, Goold RG, Wood-Kaczmar A, Gordon-Weeks PR. Glycogen synthase kinase-3 beta phosphorylation of MAP1B at Ser1260 and Thr1265 is spatially restricted to growing axons. J Cell Sci 2005;118:993–1005.
40. Zhou BP, Deng J, Xia W, Xu J, Li YM, Gunduz M, Hung MC. Dual regulation of Snail by GSK-3beta-mediated phosphorylation in control of epithelial-mesenchymal transition. Nat Cell Biol 2004; 6:931–940.

Received May 17, 2006. Accepted October 5, 2006.

Address requests for reprints to: Mamoru Watanabe, MD, PhD, Department of Gastroenterology and Hepatology, Graduate School, Tokyo Medical and Dental University, 1-5-45, Yushima, Bunkyo-ku, Tokyo 113-8519, Japan. e-mail: mamoru.gast@tmd.ac.jp.

Supported in part by grants-in-aid for Scientific Research, Scientific Research on Priority Areas, Exploratory Research, and Creative Scientific Research from the Japanese Ministry of Education, Culture, Sports, Science and Technology; the Japanese Ministry of Health, Labor and Welfare; the Japan Medical Association; the Foundation for Advancement of International Science; Terumo Life Science Foundation; Ohyama Health Foundation; Yakult Bio-Science Foundation; and the Research Fund of Mitsukoshi Health and Welfare Foundation.

The authors thank Dr Akira Kikuchi (Hiroshima University), Dr Hiroshi Shibuya (Tokyo Medical and Dental University), and Dr Keiji Tanaka (Tokyo Metropolitan Institute) for technical advice.

Research article

Unique CD14+ intestinal macrophages contribute to the pathogenesis of Crohn disease via IL-23/IFN-γ axis

Nobuhiko Kamada,[1] Tadakazu Hisamatsu,[1] Susumu Okamoto,[1] Hiroshi Chinen,[1] Taku Kobayashi,[1] Toshiro Sato,[1] Atsushi Sakuraba,[1] Mina T. Kitazume,[1] Akira Sugita,[2] Kazutaka Koganei,[2] Kiyoko S. Akagawa,[3] and Toshifumi Hibi[1]

[1]Division of Gastroenterology and Hepatology, Department of Internal Medicine, Keio University School of Medicine, Tokyo, Japan. [2]Department of Surgery, Yokohama City Hospital, Yokohama, Japan. [3]Department of Immunology, National Institute of Infectious Diseases, Tokyo, Japan.

Intestinal macrophages play a central role in regulation of immune responses against commensal bacteria. In general, intestinal macrophages lack the expression of innate-immune receptor CD14 and do not produce proinflammatory cytokines against commensal bacteria. In this study, we identified what we believe to be a unique macrophage subset in human intestine. This subset expressed both macrophage (CD14, CD33, CD68) and DC markers (CD205, CD209) and produced larger amounts of proinflammatory cytokines, such as IL-23, TNF-α, and IL-6, than typical intestinal resident macrophages (CD14$^-$CD33$^+$ macrophages). In patients with Crohn disease (CD), the number of these CD14$^+$ macrophages were significantly increased compared with normal control subjects. In addition to increased numbers of cells, these cells also produced larger amounts of IL-23 and TNF-α compared with those in normal controls or patients with ulcerative colitis. In addition, the CD14$^+$ macrophages contributed to IFN-γ production rather than IL-17 production by lamina propria mononuclear cells (LPMCs) dependent on IL-23 and TNF-α. Furthermore, the IFN-γ produced by LPMCs triggered further abnormal macrophage differentiation with an IL-23–hyperproducing phenotype. Collectively, these data suggest that this IL-23/IFN-γ–positive feedback loop induced by abnormal intestinal macrophages contributes to the pathogenesis of chronic intestinal inflammation in patients with CD.

Introduction

Although the precise etiologies of inflammatory bowel diseases (IBDs), including Crohn disease (CD) and ulcerative colitis (UC), remain unclear, several reports have indicated that dysfunction of the mucosal immune system plays important roles in its pathogenesis (1, 2). It has been suggested that skewed Th1 immune responses, represented by IFN-γ, TNF-α, and IL-2, in the inflamed mucosa, play a pivotal role in the pathogenesis of CD (3, 4). Recently, it has become evident that abnormal innate-immune responses to commensal bacteria are responsible for the pathogenesis of CD (5).

Macrophages, the major population of tissue-resident mononuclear phagocytes, play key roles in bacterial recognition and elimination as well as in the polarization of innate and adaptive immunities. Besides these classical antibacterial immune roles, it has recently become evident that macrophages also play important roles in homeostasis maintenance, for example, inflammation dampening via the production of antiinflammatory cytokines such as IL-10 and TGF-β, debris scavenging, angiogenesis, and wound repair (6–8). Since the intestinal mucosa of the gut is always exposed to numerous commensal bacteria, it is considered that the gut may possess regulatory mechanisms preventing excessive inflammatory responses against commensal bacteria. Indeed, it was previously reported that human intestinal macrophages do not express innate response receptors (9, 10), and although these cells retain their phagocytic and bacteriocidal functions, they do not produce proinflammatory cytokines in response to several inflammatory stimuli, including microbial components (11). In addition, a recent study also revealed that intestinal macrophage expressed several antiinflammatory molecules, including IL-10, and induced the differentiation of Foxp3$^+$ Treg by a mechanism dependent on IL-10 and retinoic acid. Moreover, such intestinal macrophage suppresses the intestinal DC-derived Th1 and Th17 immunity dependent on or independent of Treg induction (12). Thus, recent studies have suggested that macrophages located in the intestinal mucosa play important roles in the maintenance of intestinal homeostasis by protecting the host from foreign pathogens and negatively regulating excess immune responses to commensals (13). On the other hand, disorders in such antiinflammatory functions of intestinal macrophages may cause abnormal immune responses to commensals and lead to the development of chronic intestinal inflammation, such as IBD (14–19). In fact, intestinal macrophages contributed to the development of Th1- and Th17-mediated chronic colitis via the production of both IL-12 and IL-23 in response to commensal bacteria in IL-10–deficient mice, an animal model of CD (20). In the present study, we focused on the functions of human intestinal macrophages to clarify their role in the pathogenesis of CD.

Results

Presence of unique proinflammatory CD14$^+$ macrophages in the intestinal lamina propria. To identify the role of intestinal macrophage in the pathogenesis of human IBD, we first analyzed the macrophage population in the human intestine. Although many previous reports have indicated that CD14 is downregulated in intestinal

Nonstandard abbreviations used: CD, Crohn disease; CM, conditioned media; IBD, inflammatory bowel disease; LP, lamina propria; LPMC, LP mononuclear cell; PB, peripheral blood; UC, ulcerative colitis.

Conflict of interest: The authors have declared that no conflict of interest exists.

Citation for this article: *J. Clin. Invest.* **118**:2269–2280 (2008). doi:10.1172/JCI34610.

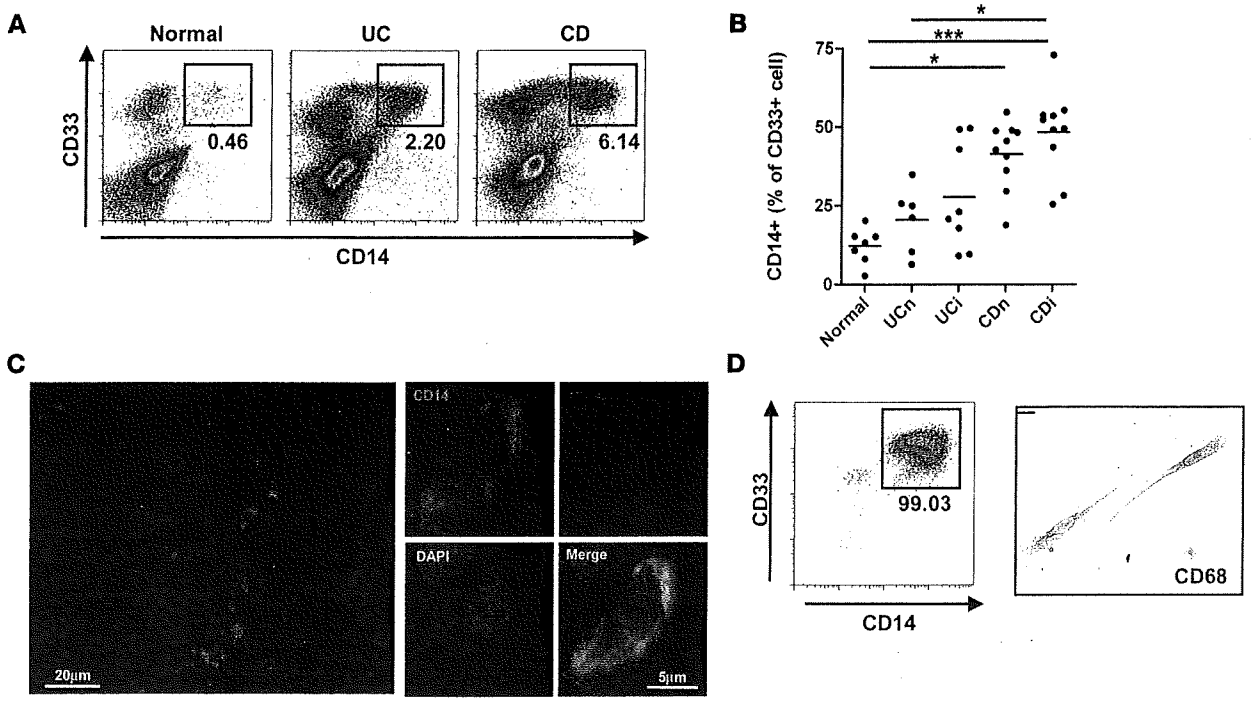

Figure 1

CD14-expressing cells were increased in the intestinal mucosa of patients with IBD. (**A**) LP macrophages of normal intestinal tissue specimens and of patients with active IBD were analyzed by FACS for CD14 and CD33 cell-surface expression. Numbers indicate the percentage of $CD14^+$ cells present in human tissue. (**B**) Percentage of $CD14^+$ intestinal macrophages among $CD33^+$ cells from normal control subjects, noninflamed mucosa of patients with UC (UCn), inflamed mucosa of patients with UC (UCi), noninflamed mucosa of patients with CD (CDn), and inflamed mucosa of patients with CD (CDi). $^*P < 0.05$, $^{***}P < 0.001$. (**C**) Fluorescence microscopy of human intestine from CD patients stained with anti-CD14 (green), anti-CD68 (red), and DAPI (blue). $CD14^+CD68^+$ macrophages were present in the intestinal LP. $CD14^-CD68^+$ macrophages were also observed. (**D**) Sorted $CD14^+CD33^+$ intestinal macrophages were analyzed for the expression of CD14 and CD33, and these cells were reseeded and analyzed for CD68. Numbers indicate the percentage of $CD14^+$ cells per sorted cells. Scale bar: 20 μm.

macrophages (9, 11), a small number of $CD14^+$ cells positive for the intestinal macrophage marker CD33 were present in normal human intestine (Figure 1A). Moreover, these $CD14^+$ cells were significantly increased in the patients with IBDs, especially in the patient with CD (Figure 1, A and B). On the other hand, there were no significant differences in the number of $CD14^+$ cells between noninflamed and inflamed mucosa in individual patients (Figure 1B). To clarify whether these cells were a new subset of intestinal macrophages or newly recruited monocytes, morphology and macrophage marker expression were assessed on both tissue localized and purified $CD14^+$ cells from the intestinal mucosa of patients with CD. Immunohistochemical analysis revealed that the $CD14^+$ cells also expressed macrophage marker CD68 (Figure 1C), and the purified $CD14^+$ cells were adherent and showed spindle-like typical macrophage morphology (Figure 1D).

Next, we analyzed the phenotype of these $CD14^+CD33^+$ cells. These $CD14^+CD33^+$ cells expressed CD13, HLA-DR, Fc receptors (CD32, CD64), transferrin receptor (CD71), mannose receptor (CD206), and IL-3 receptor (CD123) but did not express the CD16 or DC markers CD1a, CD1c, and DC-LAMP (CD208). However, this subset expressed some DC markers such as DEC-205 (CD205) and DC-SIGN (CD209) and the costimulatory molecules CD80, CD86, CD40, and TLRs (Figure 2A and Supplemental Figure 1; supplemental material available online with this article; doi:10.1172/JCI34610DS1). In addition, $CD14^+CD33^+$ cells expressed several chemokine receptors such as CCR1, -2, -4, -9, CXCR4, and CX_3CR1 (Figure 2A). In terms of the expression of surface markers, there were no marked differences among the $CD14^+CD33^+$ cells from normal control subjects and 2 types of IBD patients, at least among those subjects we tested (data not shown). On the other hand, consistent with previous reports, the $CD14^-CD33^+$ subset did not express most macrophage and DC markers (Figure 2A). Thus, these $CD14^+$ cells are thought to be a unique macrophage subset in intestine, which has both macrophage and DC markers.

Because this $CD14^+$ unique myeloid cell subset was increased in IBD patients, there is a possibility that these cells contributed to the intestinal inflammation. To clarify this, $CD14^+CD33^+$ and $CD14^-CD33^+$ cells were isolated from the lamina propria (LP) of CD patients, and the cytokine productive function after stimulation with commensal bacteria *Escherichia coli* and *Enterococcus faecalis* was assessed. $CD14^+CD33^+$ cells produced larger amounts of proinflammatory cytokines IL-12/IL-23p40, IL-23, TNF-α, and IL-6, but not IL-12p70, in response to bacterial stimuli. In contrast, $CD14^-CD33^+$ cells produced only limited amounts of these proinflammatory cytokines (Figure 2B). Even in the production of antiinflammatory cytokines, $CD14^+CD33^+$ cells produced a larger amount of IL-10 than $CD14^-CD33^+$ cells, and both subsets could produce only limited amount of TGF-β. These results suggest that $CD14^+CD33^+$ intestinal macrophage subsets act as a proinflammatory subset in the pathogenesis of human IBD.

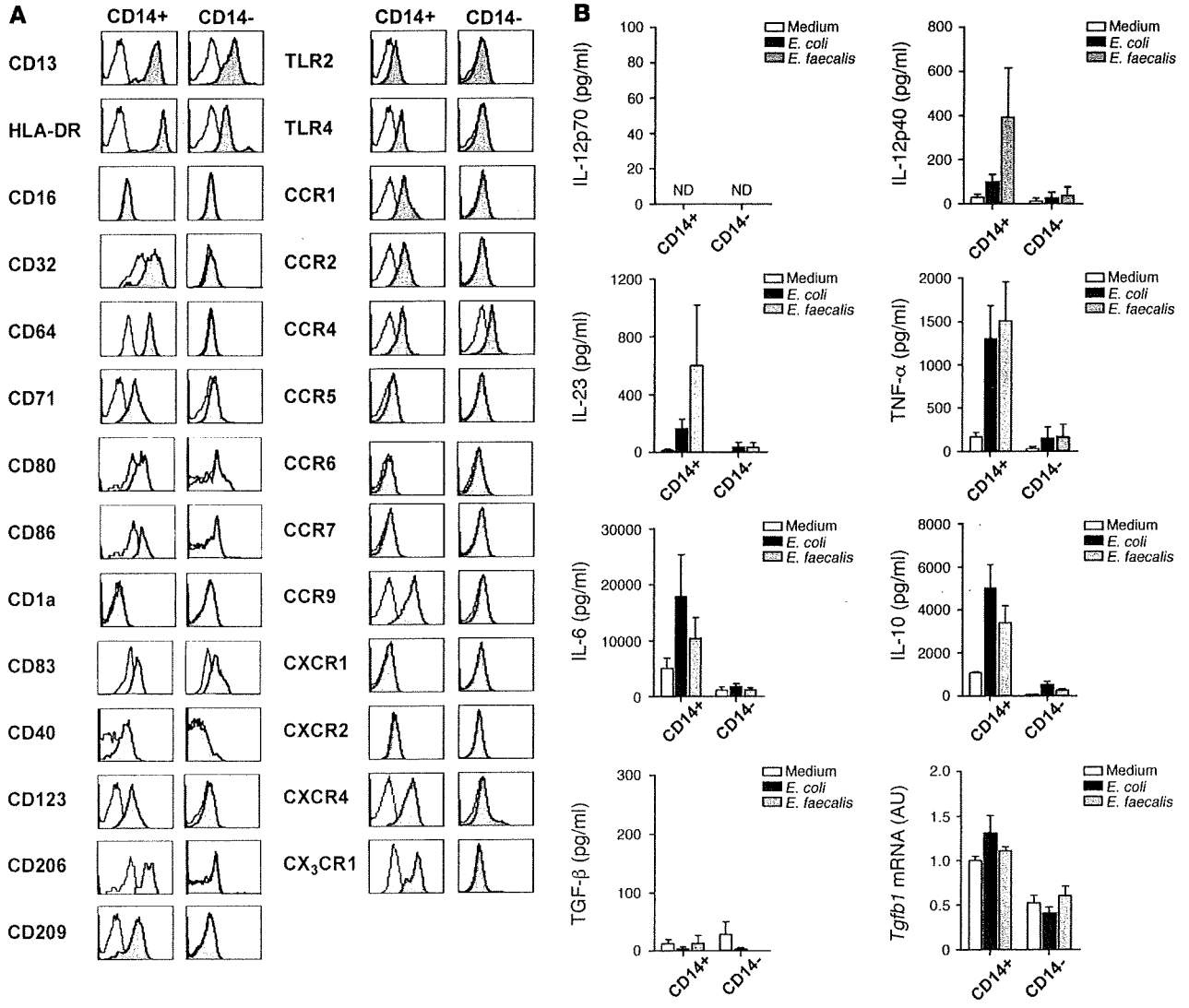

Figure 2

CD14+CD33+ cells in the human intestinal LP revealed unique phenotypes and produced larger amounts of proinflammatory cytokines than CD14−CD33+ intestinal macrophages. (**A**) Flow cytometry for the surface phenotypes of intestinal CD14+CD33+ and CD14−CD33+ cells. The shaded histogram shows the profiles of the indicated Ab staining and the open histogram shows staining with isotype controls. The data shown are representative of 5 independent experiments on normal control subjects or noninflamed mucosa of CD patients. (**B**) Proinflammatory cytokine production by *E. coli* or *E. faecalis* heat-killed antigen-stimulated CD14+CD33+ or CD14−CD33+ intestinal macrophages from the inflamed mucosa of CD patients. Control stimulation used is cell culture medium alone. N.D., not detected. Data represent mean ± SEM from at least 3 independent experiments.

CD14+ intestinal macrophages in patients with CD produce a large amount of IL-23 and TNF-α in response to commensal bacteria. Since the number of CD14+ macrophages was significantly increased in intestinal tissues from IBD patients, especially in CD patients, we next examined whether these CD14+ cells in CD patients were only increased in numbers or exhibited functional differences compared with normal controls and UC patients. We first analyzed the expression of IL-12–related genes by isolated CD14+ macrophages from normal control subjects or patients with IBD. As a result, the levels of IL-12/IL-23p40, IL-23p19, and IL-27p28, but not IL-12p35, were significantly increased in CD14+ macrophages from CD patients compared with those from normal individuals and patients with UC (Figure 3A). Moreover, in response to commensal bacteria stimulation, CD14+ intestinal macrophages from CD patients produced abundant levels of IL-23 and TNF-α, but not IL-12p70, compared with those from normal individuals and UC patients (Figure 3, B and C). CD14+ macrophages from the CD patient also produced IL-6, but the level was lower than that in UC patients (Figure 3B). Thus, the CD14+ intestinal macrophages in CD patients are distinct from those in normal and UC patients, being hyperproducers of IL-23 but not IL-12.

CD14+ intestinal macrophages in CD patients are a main source of commensal-induced IL-23 by LPMCs. It has become clear that CD14+ macrophages from patients with CD produced abundant levels of IL-23. Next, we tried to identify the role of these IL-23–producing CD14+ intestinal macrophages in intestinal inflammation. To clarify the role of these macrophage subsets in the intestinal inflammation, whole LPMCs in a mixed culture system were used for evaluation

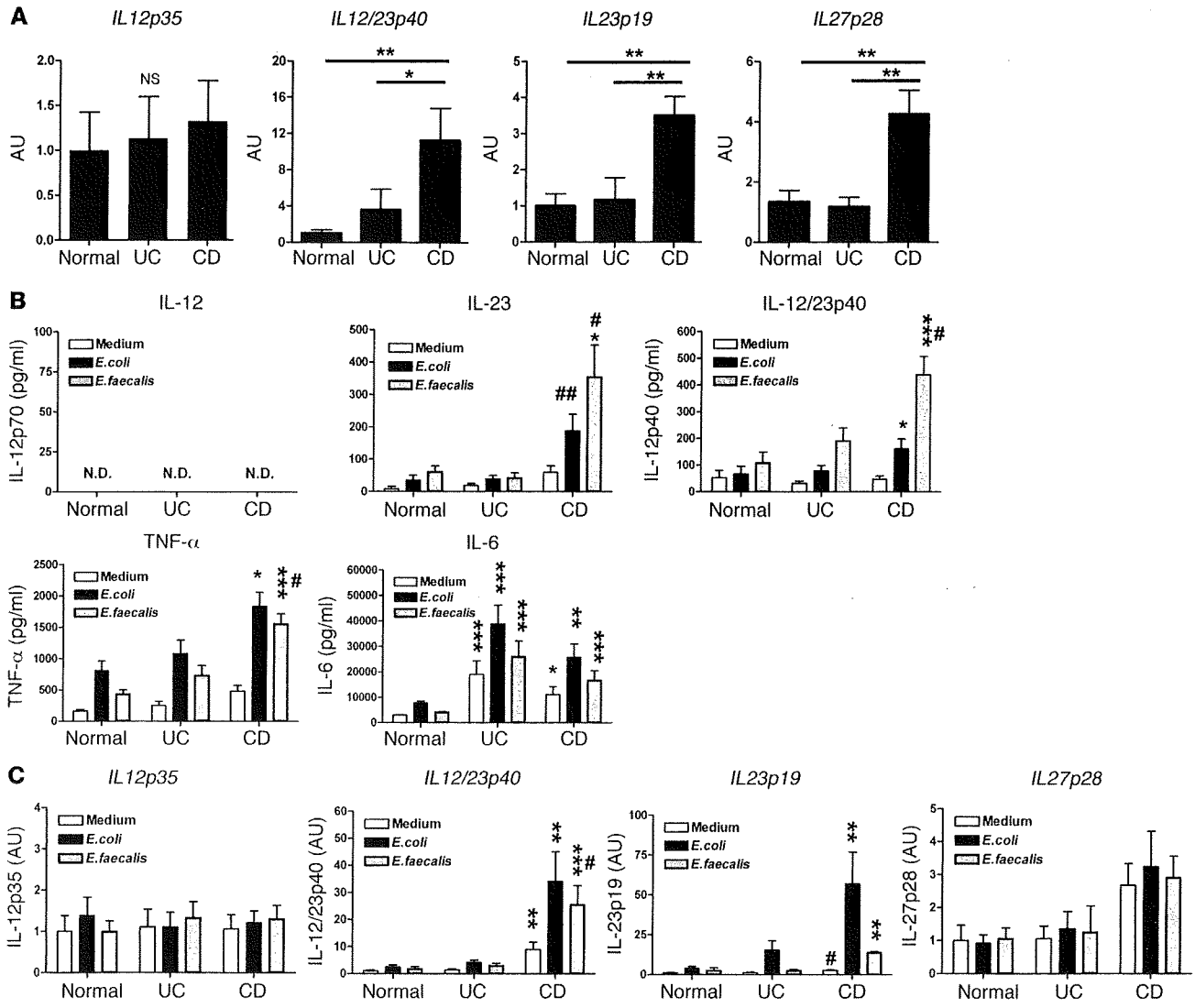

Figure 3

CD14+ intestinal macrophages from patients with CD produced abundant levels of IL-23 and TNF-α in response to commensal bacteria antigen stimulation. (**A**) Quantitative RT-PCR of basal mRNA expression levels in isolated CD14+ macrophages from normal and IBD patients. (**B**) Cytokine production by CD14+ intestinal macrophages stimulated by heat-killed *E. coli* or *E. faecalis* (1×10^8 CFU/ml) for 24 hours. (**C**) Quantitative RT-PCR of IL-12–related cytokines by CD14+ intestinal macrophages stimulated by heat-killed *E. coli* or *E. faecalis* (1×10^8 CFU/ml) for 24 hours. All CD14+ macrophages used in this experiment are from inflamed mucosa of IBD patients and noninflamed mucosa of normal control subjects. Data are expressed as mean ± SEM of individual patients or controls (normal, $n = 9$; UC, $n = 9$; CD, $n = 13$). Statistical analysis was performed using Kruskal-Wallis 1-way ANOVA and the Tukey-Kramer test for multiple comparisons. $^*P < 0.05$, $^{**}P < 0.01$, $^{***}P < 0.001$ versus normal control subjects; $^{\#}P < 0.05$, $^{\#\#}P < 0.01$ versus UC.

of macrophage-lymphocyte interaction. Intestinal LPMCs were isolated from inflamed mucosa of UC and CD patients or normal colon, respectively, and cultured with or without commensal bacteria stimulation. As shown in Figure 4A, commensal bacteria *E. faecalis* strongly induced the production of IL-23, TNF-α, and IL-6, but not IL-12p70, from LPMCs from patients with CD. Interestingly, TNF-α, which strongly contributes to the intestinal inflammation of CD, was constitutively produced to a greater extent by LPMCs from CD patients. In addition, not only proinflammatory cytokines TNF-α and IL-6, which are mainly produced by innate-immune cells, but T cell–related cytokines, such as IFN-γ, were also significantly elevated in LPMCs from CD patients both before and after bacteria stimulation (Figure 4A). Surprisingly, although the Th17-related cytokine IL-23 was significantly induced in LPMCs from patients with CD, IL-17 production was not induced by LPMCs even after bacteria stimulation. We further checked the mRNA transcription promoted by commensal stimulation. Consistent with the results of protein secretion, commensal bacteria significantly upregulated the expression of *IL12/IL23p40*, *IL23p19*, and *IFNG* mRNA; however, stimulation did not induce *IL12p35* and *IL17* mRNA in LPMCs from CD patients (Figure 4B). In contrast to *IL17*, the other Th17-related cytokines *IL22* and *CCL20* were significantly induced by LPMCs from CD patients after commensal stimulation (Figure 4B). To further confirm the

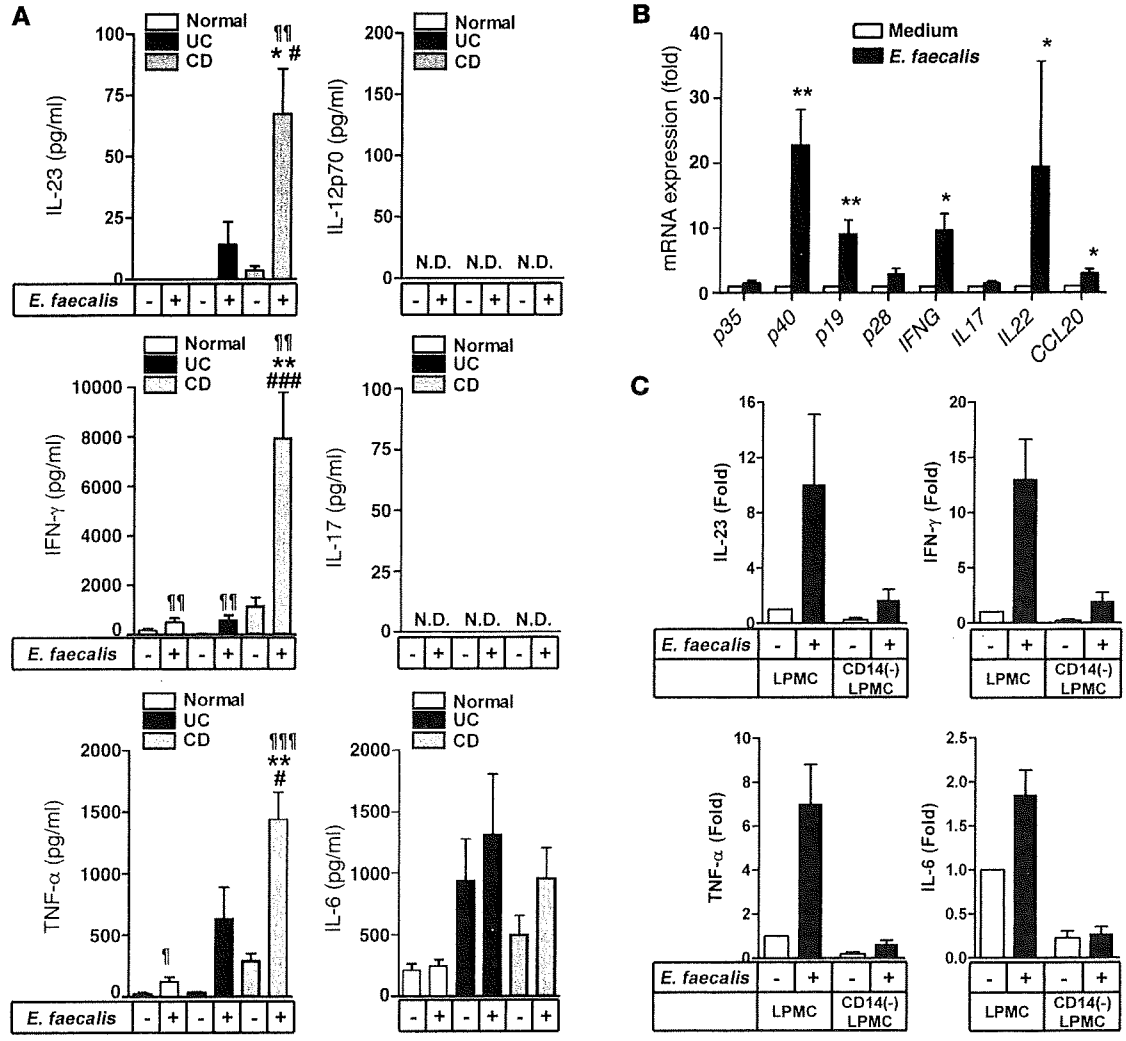

Figure 4

Commensal bacteria induced IFN-γ but not IL-17 by LPMCs via IL-23 produced by CD14⁺ intestinal macrophages. (**A**) Th1 and Th17 cytokine production by LPMCs (1×10^6 cells/ml) treated with heat-killed *E. faecalis* antigen for 24 hours. Data represent mean ± SEM (normal control, $n = 5$; UC, $n = 8$; CD, $n = 8$). LPMCs of IBD patients were isolated from inflamed mucosa both in UC and CD. Statistical analysis was performed using Kruskal-Wallis 1-way ANOVA and the Tukey-Kramer test for multiple comparisons. $^{*}P < 0.05$, $^{**}P < 0.01$ versus normal control; $^{\#}P < 0.05$, $^{\#\#\#}P < 0.001$ versus UC; $^{¶}P < 0.05$, $^{¶¶}P < 0.01$, $^{¶¶¶}P < 0.001$ versus unstimulated controls. (**B**) Th1- and Th17-related cytokine mRNA expression after commensal bacteria stimulation (12 hours) by LPMCs from inflamed mucosa of patients with CD. Data represent mean ± SEM of at least 6 individuals. p35, *IL12p35*; p40, *IL12/IL23p40*; p19, *IL23p19*; p28, *IL27p28*. Statistical analysis was performed using Wilcoxon test. $^{*}P < 0.05$, $^{**}P < 0.01$. (**C**) Basal and commensal-induced cytokine production by LPMCs or CD14⁺ cells depleted LPMCs from inflamed mucosa of patients with CD. Data represent mean ± SEM from 6 independent experiments.

CD14⁺ cells as the major source of IL-23, the CD14⁺ cells were depleted from LPMCs, and then CD14⁻ LPMCs were stimulated with *E. faecalis*. As expected, the production of proinflammatory cytokines IL-23, TNF-α, and IL-6 was dramatically reduced in CD14⁻ LPMCs compared with whole LPMCs (Figure 4C). Because this reduction of cytokines by LPMCs was not due to the nonspecific cell damage caused by CD14⁺ cell depletion (Supplemental Figure 4), it seems likely that these phenomena were caused by the lack of CD14⁺ macrophages from LPMCs. Moreover, IFN-γ production was also dramatically decreased in the CD14⁻ LPMCs (Figure 4C). Because CD4⁺ T cells are a major source of IFN-γ in the inflamed mucosa of CD patients (3, 4) and CD14⁺ cells could not produce IFN-γ (data not shown), IFN-γ was thought to be produced by T cells as a result of the interaction with bacteria-activated innate-immune cells, such as macrophages, in the LPMCs.

Collectively, these results suggest that CD14⁺ macrophages were the major source of IL-23 in the LP of CD patients and might have contributed to the promotion of IFN-γ production from LP T cells.

CD14⁺ intestinal macrophages in CD patients promote IFN-γ, rather than IL-17, by LP T cells via an IL-23– and TNF-α–dependent manner. To unravel the role of IL-23, which is produced by CD14⁺ intestinal macrophages, we examined the effect of IL-23 on the intestinal inflammatory response using LPMC cultures. Consistent with the results of commensal bacteria stimulation, recombinant IL-23 (rIL-23) significantly induced IFN-γ, but not IL-17, production by LPMCs. Indeed, the amounts of IFN-γ were dramatically higher in

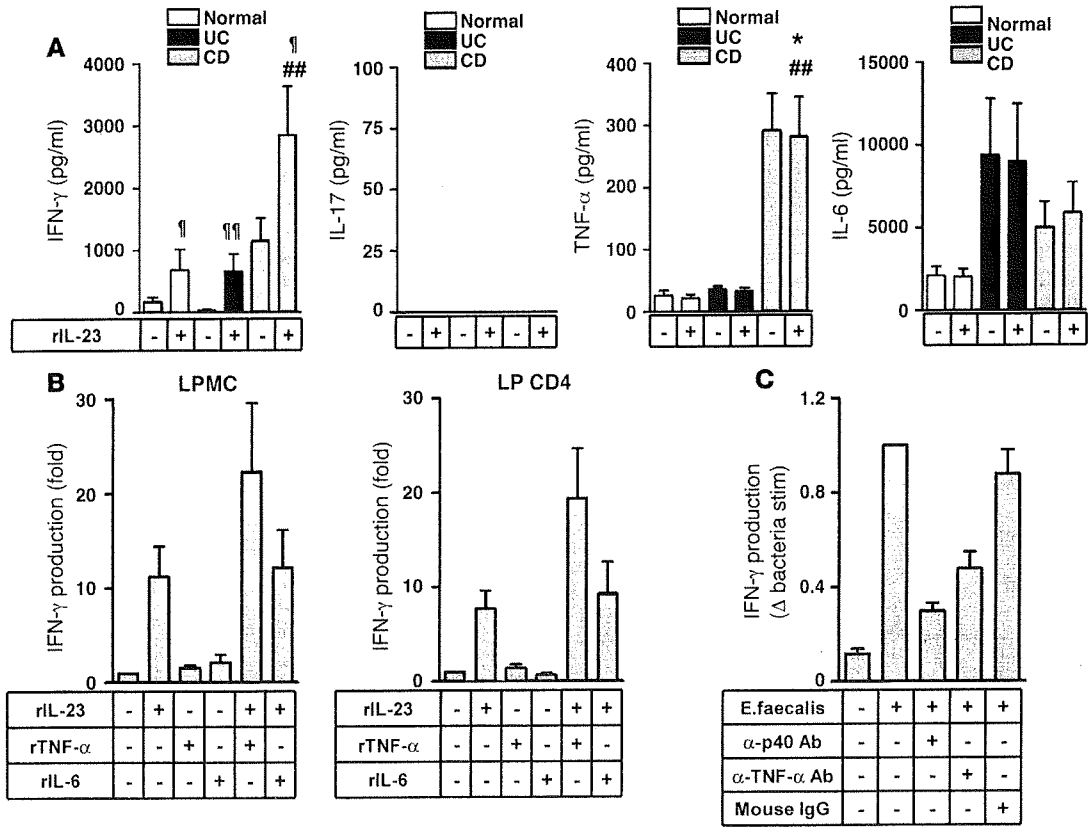

Figure 5

Intestinal macrophage-derived IL-23 induced IFN-γ production by LPMCs, and LP CD4+ T cells synergize with TNF-α in patients with CD. (**A**) IL-23–induced proinflammatory cytokine production by LPMCs from normal control subject or inflamed mucosa of patients with IBD. Data represent mean ± SEM (normal control, $n = 5$; UC, $n = 8$; CD, $n = 8$). $^{*}P < 0.05$ versus normal control; $^{\#\#}P < 0.01$ versus UC; $^{¶}P < 0.05$, $^{¶¶}P < 0.01$ versus unstimulated controls. (**B**) Synergistic effect of TNF-α and IL-6 on the IL-23–induced IFN-γ production by LPMCs and LP CD4+ T cells from inflamed mucosa of patients with CD. Data represent mean ± SEM from 4 individuals. (**C**) Analysis of the suppressive effect of anti-p40 or anti–TNF-α Abs on the commensal bacteria-induced IFN-γ production by LPMCs from inflamed mucosa of CD patients. α-p40 Ab, α–IL-12/IL-23p40 Ab. Data represent mean ± SEM from at least 4 individuals. Statistical analysis was performed using Kruskal-Wallis 1-way ANOVA and the Tukey-Kramer test for multiple comparisons.

patients with CD than in normal control subjects or patients with UC (Figure 5A). While rIL-23 significantly promoted the production of IFN-γ by LPMCs, the amount of commensal-promoted IFN-γ was 2-fold larger than that of rIL-23–promoted IFN-γ, especially in CD patients (Figure 4A and Figure 5A). To explain this difference, we focused on the possibility that other proinflammatory cytokines exhibit synergistic effects with IL-23 on IFN-γ induction by LPMCs. Commensal bacteria stimulation induced not only IL-23 but also TNF-α and IL-6, while IL-23 alone did not induce such proinflammatory cytokines. Hence, there is a possibility that IL-23 and TNF-α or IL-6 can act synergistically on IFN-γ induction. As shown in Figure 5B, both TNF-α and IL-6 did not induce IFN-γ production by LPMCs and LP T cells. However, TNF-α, but not IL-6, synergistically induced IFN-γ from LPMCs and LP CD4+ T cells with IL-23. Indeed, commensal bacteria-induced IFN-γ by LPMCs was suppressed by neutralizing IL-12/IL-23p40 and TNF-α (Figure 5C). Thus, bacteria-induced TNF-α may act in cooperation with IL-23 on IFN-γ induction in the intestinal inflammatory site in CD patients. Collectively, CD14+ macrophages are a major producer of IL-23 and TNF-α in the intestinal LP of CD patients. Such IL-23 and TNF-α synergistically induce the production of IFN-γ by LP T cells.

The intestinal inflammatory microenvironment in CD patients promotes abnormal differentiation of intestinal macrophage. As we have demonstrated so far, an abnormal macrophage subset might contribute to the pathogenesis of intestinal inflammation of CD patients via IL-23 overproduction. In the next part of this study, we tried to identify how such abnormal intestinal macrophage differentiation is triggered in CD patients. We hypothesized that local inflammatory microenvironments in CD patients might cause abnormal macrophage differentiation. To examine this hypothesis, conditioned media (CM) were prepared from whole-cell cultures of intestinal LPMCs from normal subjects and patients with IBD, without stimulation. Then, the effect of LPMC-CM was assessed using an in vitro macrophage differentiation system. Peripheral blood (PB) CD14+ monocytes were obtained from healthy donors and differentiated into macrophage by M-CSF with or without LPMC-CM. There was no significant difference in morphology (Figure 6A), but the expression of cell-surface markers was different among the differentiated cells (Figure 6B). M-CSF–induced macrophages expressed CD14 and CD33 but not CD209 and CD206. Alternatively, CM-derived macrophages expressed all of these markers regardless of the source of CM, and the phenotype was similar to

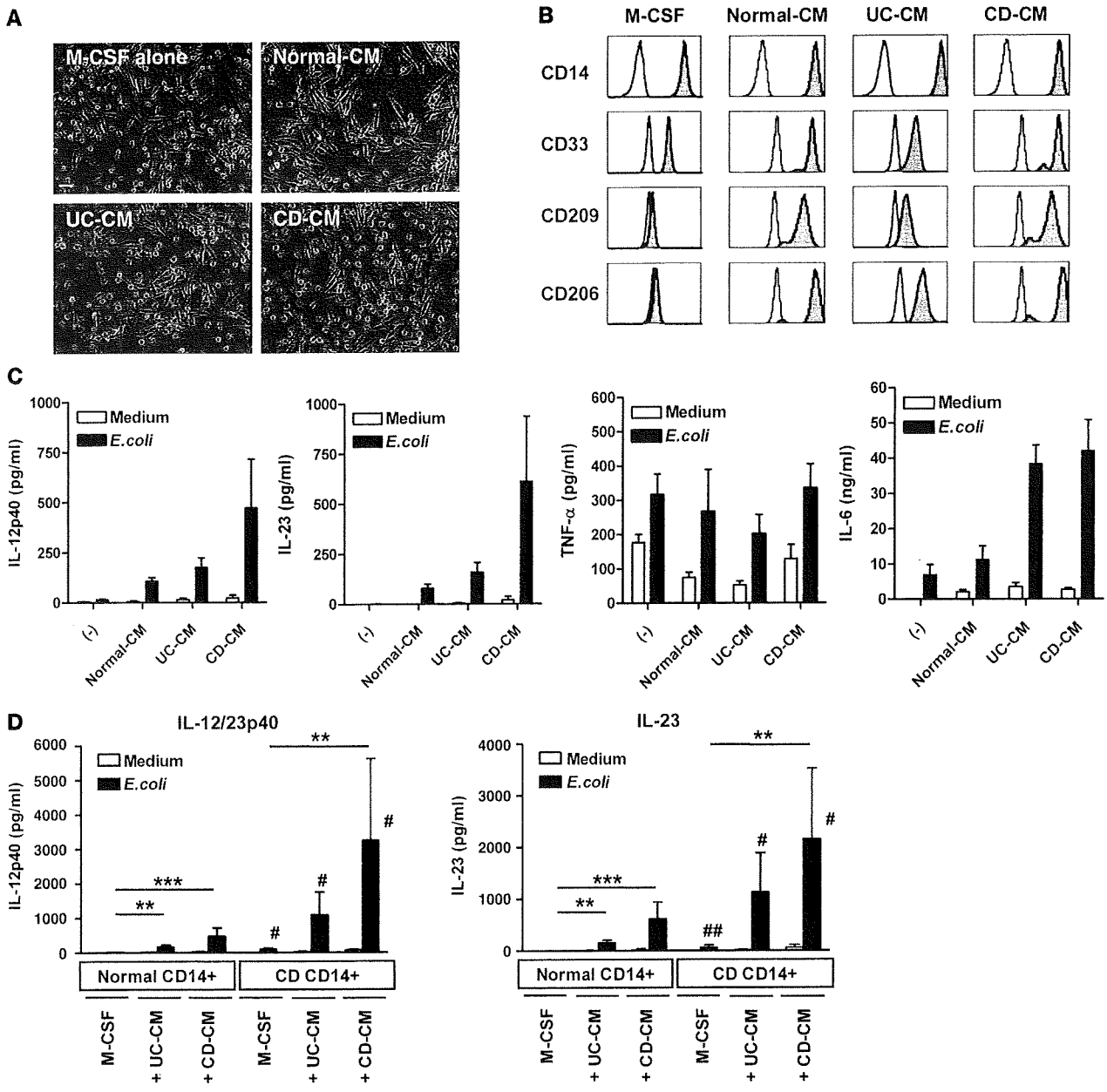

Figure 6

The intestinal inflammatory microenvironment affects macrophage differentiation and induces an IL-23–producing phenotype. (**A**) Morphological findings of in vitro–differentiated macrophages from peripheral CD14+ monocytes of normal controls with or without LPMC-CM. Scale bar: 20 μm. (**B**) Flow cytometry for the surface phenotypes of LPMC-CM–induced in vitro–differentiated macrophages. The shaded histogram shows profiles of indicated Ab staining and the open histogram shows staining with isotype controls. The data shown are representative of 5 independent experiments. (**C**) Cytokine production by LPMC-CM–induced in vitro–differentiated macrophages stimulated with heat-killed *E. coli* for 24 hours. Data represent mean ± SEM from 6 independent experiments. (**D**) Cytokine production by macrophages differentiated from normal and CD monocytes with or without UC- and CD-CM. Data represent mean ± SEM from 5 independent experiments. All data used at least 3 different CM from individual patients and at least 3 different monocytes from individual patients and controls. Statistical analysis was performed using Kruskal-Wallis 1-way ANOVA and the Tukey-Kramer test for multiple comparisons. $^{**}P < 0.01$, $^{***}P < 0.001$ versus M-CSF induced macrophages; $^{\#}P < 0.01$, $^{\#\#}P < 0.01$ comparison between normal control monocytes and monocytes from CD patients.

that of intestinal macrophages. However, production of IL-23 and IL-12/IL-23p40 by these macrophages was significantly different and clearly higher in CD-CM–induced macrophages, as shown in Figure 6, C and D. Thus, it seems possible that CD-CM specifically affects monocyte differentiation, at least on the cytokine production ability, and induces IL-23–hyperproducing macrophages. These results indicate that the inflammatory microenvironment of intestinal mucosa in patients with CD affected macrophage differentiation and altered their phenotype to abnormal macrophages with an IL-23–hyperproducing phenotype. Then, we tried

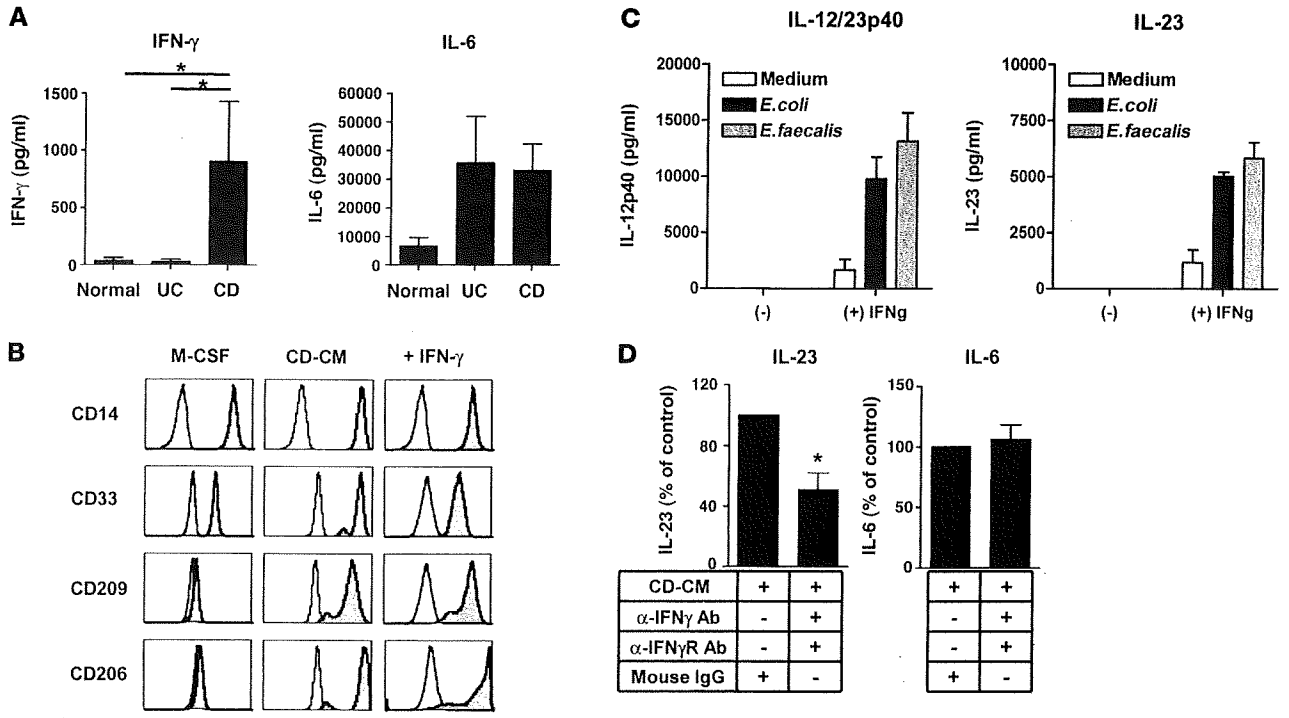

Figure 7

IFN-γ in CD-CM promotes IL-23–hyperproducing proinflammatory macrophage differentiation. (**A**) Quantification of IFN-γ and IL-6 in LPMC-CM. Data are shown as mean ± SEM from 3 individual normal controls and 4 individual patients with IBD used for macrophage differentiation experiments. (**B**) Flow cytometry for the surface phenotypes of IFN-γ–induced in vitro–differentiated macrophages. The shaded histogram shows the profiles of the indicated Ab staining and the open histogram shows staining with isotype controls. (**C**) Production of IL-12/IL-23p40 and IL-23 by bacteria-stimulated macrophages differentiated with or without IFN-γ. Data represent mean ± SEM from 3 independent experiments. (**D**) Effect of IFN-γ signal blocking using anti–IFN-γ Ab (α-IFNγ Ab) (1 μg/ml) combination with anti–IFN-γ receptor 1 Ab (α-IFNγR Ab) (10 μg/ml) or same amount of those isotype controls (mouse IgG; mouse IgG_{2A} for α-IFNγ Ab, and mouse IgG_1 for α-IFNγR Ab) from CD-CM on macrophage differentiation. Statistical analysis was performed using paired *t* test. Data represent mean ± SEM from 5 independent experiments. $^*P < 0.05$ compared with controls.

to determine whether only inflammatory conditions affected macrophage differentiation or if CD patients have some abnormalities in monocytes. To address this issue, monocytes from patients with CD were used for in vitro macrophage differentiation with UC- or CD-CM. Compared with normal monocyte-derived macrophages, CD monocyte–derived macrophages produced more IL-23 in response to bacterial stimuli. These results suggest that CD monocytes are distinct from normal monocytes and are more susceptible to CD-CM and altered their phenotype into IL-23 hyperproducers (Figure 6D).

IFN-γ in CD-CM leads to abnormal macrophage differentiation with an IL-23–hyperproducing phenotype. As described above, it has become evident that intestinal microenvironments in patients with CD lead to abnormal macrophage differentiation with an IL-23–hyperproducing phenotype. However, it was still unclear which factors in CD-CMs cause abnormal macrophage differentiation. As shown in Figure 4, some proinflammatory cytokines, such as IFN-γ and TNF-α, were spontaneously produced by LPMCs after culture for 24 hours, especially in CD patients. Hence, we focused on the effect of such proinflammatory cytokines on macrophage differentiation. To identify these factors, the cytokines in CD-CM were analyzed. In fact, the amount of IFN-γ was highest in CD-CM among normal-, UC-, and CD-CM groups (Figure 7A). In contrast, other proinflammatory cytokines, such as IL-6, were elevated in both CD- and UC-CM (Figure 7A). Unexpectedly, in contrast to the results in Figure 4, all LPMC-CMs used in this study did not contain a detectable amount of TNF-α (data not shown). This difference might occur due to differences in culture times (LPMC-CMs were prepared by 60-hour culture of LPMCs in the absence of stimulation, while the result in Figure 4A revealed the cytokine amounts at 24-hour culture). Therefore, we examined the effect of recombinant IFN-γ on macrophage differentiation. IFN-γ–derived macrophages were similar to intestinal $CD14^+$ macrophages or CD-CM–derived macrophages in terms of the expression of some surface markers, and commensal bacteria stimulation induced the hyperproduction of IL-12/IL-23p40 and IL-23 (Figure 7, B and C). However, other proinflammatory cytokines, including TNF-α and IL-6, did not affect macrophage differentiation (data not shown). In addition, blocking of IFN-γ and its receptor in the culture of monocytes with CD-CM significantly, but not completely, attenuated such abnormal IL-23 production by macrophages (Figure 7D). These results indicate that IFN-γ in the CD-CM is a factor that promotes abnormal macrophage differentiation and leads to an IL-23–hyperproducing phenotype.

Discussion

It has been reported that human intestinal macrophages do not express typical macrophage innate-immune receptors, such as CD14 or TLRs, and that they exhibit antiinflammatory anergic phenotypes (9, 11). On the other hand, in IBD, it has been reported that abnormal proinflammatory macrophages, such as $TREM\text{-}1^+$ mac-

rophages, are increased in intestinal mucosa and contributed to the intestinal inflammation (19). In addition to the prior report, it was also shown that $CD14^+$ and TLR^+ myeloid cells are also increased in the LP of patients with IBD (21, 22). Thus, such innate-immune receptor–positive myeloid cells may contribute to the pathogenesis of human IBD. In the present study, we identified what we believe to be unique $CD14^+$ intestinal macrophages in the human intestinal LP. Consistent with the prior report, these cells expressed TREM-1 (Supplemental Figure 1). We also showed that the chemokine receptor expression pattern was quite different between $CD14^+CD33^+$ intestinal macrophages and $CD14^-CD33^+$ intestinal macrophages, which are considered to be the typical resident macrophages. These data suggest the possibility that these 2 intestinal macrophage subsets are derived from different subsets of monocyte, such as inflammatory or resident monocytes as previously reported (6, 23).

Moreover, the number of unique $CD14^+$ macrophage subsets was dramatically increased not only in inflamed mucosa but also in noninflamed mucosa with CD (Figure 1B). This result suggests that the increasing number of $CD14^+$ macrophages in CD patients was not simply caused as a secondary event associated with increased inflammation in CD. Moreover, not only the numbers but also the functions of this subset were dramatically changed in CD patients. The $CD14^+$ macrophage subset from CD patients produced abundant levels of IL-23 and TNF-α compared with normal control subjects and patients with UC in response to bacteria stimulation. However, it was unclear whether this enhanced IL-23 and TNF-α level produced by $CD14^+$ macrophages in CD patients plays a causal role in the inflammation of CD patients or represents a secondary event associated with increased inflammation observed in CD, because the basal production of these proinflammatory cytokines by $CD14^+$ macrophages was also higher in patients with CD. A similar unique macrophage subset has already been reported in mice. A subset of murine intestinal macrophages expressed both murine macrophage marker F4/80 and DC marker CD11c and directly induced the development of granuloma (24). In order for these unique intestinal macrophages subset in mice to develop granuloma formation, commensal bacteria-induced IL-23 is an essential factor. Based on these reports, the $CD14^+$ intestinal macrophages identified herein in humans might be a counterpart of such unique intestinal macrophages subset in mice and contribute to the development of granulomas, a typical characteristic finding in patients with CD, owing to the production of excess IL-23 and TNF-α in response to commensal bacteria.

This abnormally large amount of IL-23 observed in CD patients was induced by specific commensal bacteria, such as *E. faecalis* and *E. coli*, which were determined as colitogenic bacteria in a murine model of CD (25). In addition, stimulation with pathogen-associated molecular patterns (PAMPs) alone could not induce IL-23. Furthermore, inhibition of phagocytosis suppressed IL-23 production (Supplemental Figure 2). These findings imply that the specific species of commensal bacteria, considered to be colitogenic bacteria, strongly induce IL-23 production via intracellular recognition pathways. A recent study has demonstrated that the intracellular bacteria recognition receptor NOD2 is important for the bacteria-induced IL-23 production by monocyte-derived DCs from patients with CD (26). However, a NOD2 ligand muramyldipeptide (MDP) could not induce IL-23 by $CD14^+$ intestinal macrophages (Supplemental Figure 2D).

Because it has become evident that the IL-23/Th17 axis is more important than the IL-12/Th1 axis in various autoimmune and inflammatory diseases (27–30), including animal models of IBD (31, 32), the role of the IL-23/Th17 axis in the pathogenesis of human CD has become increasingly attractive. In fact, recent studies have suggested the existence of an IL-23 receptor polymorphism that is associated with the pathogenesis of IBD (33). In the present study, it has become clear that unique $CD14^+$ macrophages were the major source of IL-23 in the LP in response to commensal bacteria stimulation. Interestingly, these cells never produced IL-12p70. Moreover, such macrophages were not observed in PBMCs, and IL-23 did not show any effect on the production of IFN-γ or IL-17 by PBMCs or PB $CD4^+$ T cells (data not shown). Because it was previously reported that IL-23 is important for local inflammation rather than systemic inflammation, while IL-12 shows the opposite effect (34), the unique macrophage subset that we identified might play a central role in local inflammation of the gut via IL-23, but not IL-12.

In the present study, we demonstrated that IL-23 and TNF-α but not IL-6 produced by $CD14^+$ macrophages synergistically promoted IFN-γ production by LPMCs and LP $CD4^+$ T cells. Unexpectedly, however, IL-17 was not induced by LPMCs after IL-23 or commensal bacteria stimulation. In contrast, IL-17 was detected from longer-duration culture supernatants of LPMCs (48 hours and 72 hours), but the amounts were quite low and were not significantly induced with commensal bacteria stimulation (Supplemental Figure 3). These results suggest the possibility that while IL-17 contributes more to the pathogenesis of CD patients in the later phase of inflammation than IFN-γ, commensal bacteria recognition by $CD14^+$ intestinal macrophages predominantly enhances IFN-γ production rather than IL-17 production by LPMCs in patients with CD. On the other hand, we found an abundant amount of IL-17 was produced by purified LP $CD4^+$ T cells from patients with CD, both with and without TCR engagement (data not shown). These results collectively suggest the possibility that although LP $CD4^+$ T cells potentially produce both IFN-γ and IL-17, IL-17 production was suppressed in LPMCs, albeit by a largely unknown mechanism. However, we demonstrated that the other Th17-related cytokines IL-22 and CCL20 were significantly induced by LPMCs in CD patients after commensal stimulation. Thus, IL-23/Th17 immune responses were actually induced in CD patients after commensal bacteria stimulation. Since both IFN-γ and IL-17 producing cells, named Th17/Th1 cells, were identified in the patients with CD (35), there is a possibility that IL-23 induced the IFN-γ from Th17/Th1 cells rather than Th1 cells. Collectively, although IL-23 contributes to the induction of IL-17, IL-23 predominantly induces IFN-γ in the LP and leads to Th1- or Th17/Th1-mediated intestinal inflammation in CD. In agreement with our findings, although the IL-23/IL-17 axis is important in the pathogenesis of several animal models of colitis, IFN-γ production was strongly elevated (36, 37) and not only IL-17 but also IFN-γ production was markedly decreased when these mice were under IL-23–deficient conditions (38, 39). These results indicate that not only the IL-23/IL-17 axis but also the IL-23/IFN-γ axis is important for the pathogenesis of animal colitis models as well as pathogenesis of humans.

Meanwhile, it was also reported that the IL-23/IFN-γ axis was observed in both T cell dependent and independent colitis models (38). In these models, non–T cell–derived IFN-γ or IL-17 are important for colitis development. In fact, we have demonstrated that not only LP T cells but also LP $CD3^-CD56^+$ NK cells can produce IFN-γ in response to IL-23 (Supplemental Figure 5). A recent study has demonstrated that unique intestinal NK cell differentiation was accelerated in patients with CD, and such intestinal NK cells